THE COUPLED LIQUID AND GAS TRANSPORT IN A PEM FUEL CELL ELECTRODE

by

Leslie J. Fairbairn

B. Sc. Simon Fraser University, 2003

A THESIS SUBMITTED IN PARTIAL FULFILLMENT
OF THE REQUIREMENTS FOR THE DEGREE OF
MASTERS OF SCIENCE
in the Department
of
Mathematics

SIMON FRASER UNIVERSITY
June 2003

APPROVAL

Name: Leslie J. Fairbairn

Degree: Masters of Science

Title of thesis: The Coupled Liquid and Gas Transport in a PEM Fuel Cell Electrode

Examining Committee: Dr. Rustum Choksi
Chair

Dr. Keith Promislow
Supervisor
Simon Fraser University

Dr. David Muraki
Simon Fraser University

Dr. Brian Wetton
External Examiner
University of British Columbia

Date Approved: June 18, 2003

PARTIAL COPYRIGHT LICENCE

Title of Thesis/Project/Extended Essay

The Coupled Liquid and Gas Transport in a PEM Fuel Cell Electrode

Author:

(signature)

Leslie Fairbairn

(name)

August 8, 2003

(date)

Abstract

The cathode of a Proton Exchange Membrane (PEM) fuel cell serves to conduct reactant (O_2) gas to the catalyst layer, while removing by-products of the reaction, namely water in both liquid and vapour phase. This leads to delicate transport issues involving counter propagation, multi-phase flow sensitively coupled to the temperature profile through the phase change.

We develop a 1D model of this coupled liquid-gas transport in the gas diffusion layer of a PEM fuel cell electrode. We non-dimensionalize the model, indentifying scaling regimes in which the temperature and water vapour are slaved to the temperature profile at steady-state. We find that the liquid water transport is dominated by capillary pressure, that the heat transport is dominated by diffusion, while the gas transport is convectively dominated during transients but settles down to a diffusively driven steady-state.

We introduce a parameter ν whice determines the ratio of liquid water to water vapour production in the catalyst layer and tune ν so there is no boundary layer in the slaved water vapour concentration. In this regime the liquid water equation will de-couple from the gas and temperature equations when we are solving up to leading order.

We use the reduced model to examine the role of hydrophobicity on liquid water transport and the role of temperature gradients on gas transport.

Acknowledgments

I would like to extend a huge thanks to my supervisor, Keith Promislow, for all his patience, suggestions and help - I would not have written this thesis without him. Thanks as well to Jean St-Pierre from Ballard Power Systems and Brian Wetton, from UBC, for their helpful hints and encouragement. Thanks to John Stockie, from the University of New Brunswick, for all his help and for providing figures and research material for me. Thanks as well to all the members of the "Ballard" team (at Ballard Power Systems). It has been a great experience working with such a wonderful group of people.

I would also like to thank all of my office mates, in particular, Colin Macdonald, Ben Ong, Jeffrey Gilmore, Mohamed Sulman and Reza Naserasr for all their patience, friendship and the many helpful tips they have shared with me over the last two years. My experience at SFU would not have been the same without them!

A huge thanks also goes to the members of the Math Department at SFU, in particular, Dave Muraki and Bob Russell for their great instruction, patience and inspiration that they provided all of us in the Math Department.

Finally, many thanks go to my family and friends for all their encouragement, support and belief in me over the last six years.

Contents

List of Figures

Chapter 1

Introduction

The PEM (proton exchange membrane) fuel cell is an innovative and non-polluting energy conversion system. It consumes the reactant gases oxygen and hydrogen and generates useful potential voltage with water as a by-product.

The fuel cell can be used as an energy source for diverse purposes that vary from laptop computers, to generators, to car engines. The most popular focus, as fossil fuel reserves are depleted and the ozone layer decays, is to power vehicles. Unfortunately, for this purpose, pure hydrogen is difficult to transport and therefore cannot be used directly to run the fuel cell. Instead, hydrogen must be extracted from methane, which is both costly and produces such by-products as carbon-monoxide which harm the environment. Still, to run the fuel cell on methane does not produce as many toxins as the combustion engine and methane is a much more abundant fuel.

1.1 The structure of the PEM fuel cell

The PEM fuel cell is composed of five major components. The first, the outer casings, are the graphite plates. Within these graphite plates, are etched oxygen and hydrogen flow channels. Next, there are two gas diffusion layer electrodes. On one side, there is the gas diffusion layer anode, and on the other, the cathode. Next, there is a thin platinum catalyst layer on either side of the PEM between the two electrodes. Finally, between the catalyst layers, there is the polymer proton exchange membrane

which is permeable to the hydrogen protons but impermeable to its electrons. It is this membrane, along with other factors, that allows for current flow and hence for energy production in the PEM fuel cell. The GDL electrodes, catalyst layer and PEM together form what is called the MEA (membrane electrode assembly). See Fig. 1.1 (from [23]).

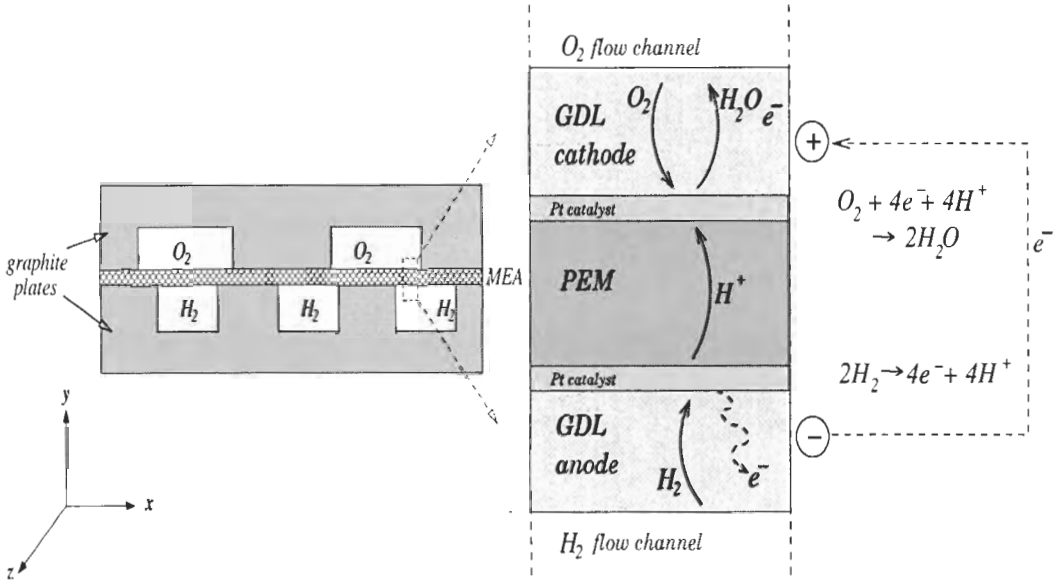

Figure 1.1: A cross-section of a PEM Fuel Cell. The MEA is surrounded by graphite plates, within which are etched the oxygen and hydrogen flow channels.

The graphite plates surround the GDL and help conduct the current generated within the fuel cell. The flow channels etched within these plates serve to transport the reactant H_2 and O_2 gases on the anode and cathode sides respectively. As well, the flow channels on the cathode side contain water in liquid and vapour form produced in the reaction at the catalyst layer.

The PEM is a polymer membrane that is permeable to the H^+ protons but not the electrons. The protons pass through the membrane to the catalyst layer on the cathode side while the electrons must pass via an external circuit to reach the catalyst layer.

The catalyst layer on either side of the PEM is comprised of platinum and other elements and is impregnated with Teflon to prevent flooding. This layer serves two

main purposes. On the anode side, it serves to facilitate the splitting of the hydrogen gas into protons (which then migrate across the PEM) and electrons. On the cathode side, it serves to facilitate the combining of oxygen, hydrogen protons and electrons to form water. The two reactions that occur on the anode and cathode sides can be written respectively as follows:

$$2H_2 \rightarrow 4e^- + 4H^+ \qquad 0_2 + 4e^- + 4H^+ \rightarrow 2H_2O$$

This separation of the reaction $2H_20 + O_2 \rightarrow 2H_2O$ into these two steps generates the useful potential energy in the PEM Fuel Cell.

Finally, the GDL electrodes (anode and cathode) are composed of a thin porous carbon fiber paper. These electrodes serve three main purposes. Firstly, they distribute the reactant oxygen and hydrogen gases uniformly to the catalyst layer. Second, they hold the catalyst layer. Third, they help eliminate the water produced at the catalyst layer on the cathode side. As well, like the graphite plate, the GDL electrodes are also made of conducting material. Like the catalyst layer, the GDL is also impregnated with Teflon to prevent flooding - which inhibits gas flow and hence the reactions in the fuel cell. We model the multiphase flow in the GDL cathode.

1.2 The key issues in PEM fuel cell modeling

The mains concern in the GDL of a fuel cell is the O_2 flux to the catalyst layer. THis is impacted by the temperature at which the fuel cell operates and the water content within the GDL. These two issues are sensitively coupled - since condensation produces heat and heat causes evaporation. The temperature in the fuel cell is a sensitive issue since too low a temperature can reduce the effect of the catalyst in the reactions and too high temperature can cause dehydration of the membrane or worse, structural damage to the fuel cell. The water content is a sensitive issue also. In order for the membrane to be conductive to H^+, it needs a certain water level. At the same time, too much water within the GDL can block the pores and inhibit hydrogen gas diffusion to the catalyst layer. The result is that the fuel cell ceases

to produce electricity. Therefore, both the temperature and water levels must be carefully controlled within the fuel cell.

Chapter 2

The Model

Let us first explain the coordinate system chosen for the model. The x-axis follows along the horizontal direction of the MEA (membrane electrode assembly). The y-axis goes in the direction through the thickness of the MEA. Finally, the z-axis follows along the length of the flow channels. (See Fig.2.1). We will present a 1D model where we examine the variations in the oxygen, water (vapour and liquid) and nitrogen concentrations as well as temperature levels in the y-direction.

In the model, we will assume that the PEM fuel cell is operating at a prescribed current, $I = 1\ amp/cm^2$. As well, as explained later on, the fuel cell is assumed to be running with the water vapour almost at saturation and there is no water cross-over to the anode side. As a result, the water vapour concentration is prescribed, which causes the boundary condition at the catalyst layer and GDL interface to be an extra constraint. To avoid a boundary layer at the catalyst layer due to this constraint, we introduce the parameter ν which specifies the percentage of water produced in the liquid form. We tune ν so that the water vapour is at saturation at the catalyst layer. This is a fairly important assumption - we are explicitly specifying the percentage of liquid water produced in the fuel cell. If ν is found to be equal to -1, there is no water vapour flux and all the product water is in liquid form. Whereas, if ν is equal to 0, there will be no liquid water flux.

We will also assume that the carbon fiber paper that comprises the GDL is homogeneous. Therefore, the void fraction within the GDL, ϵ is a constant value - $\epsilon = 0.74$

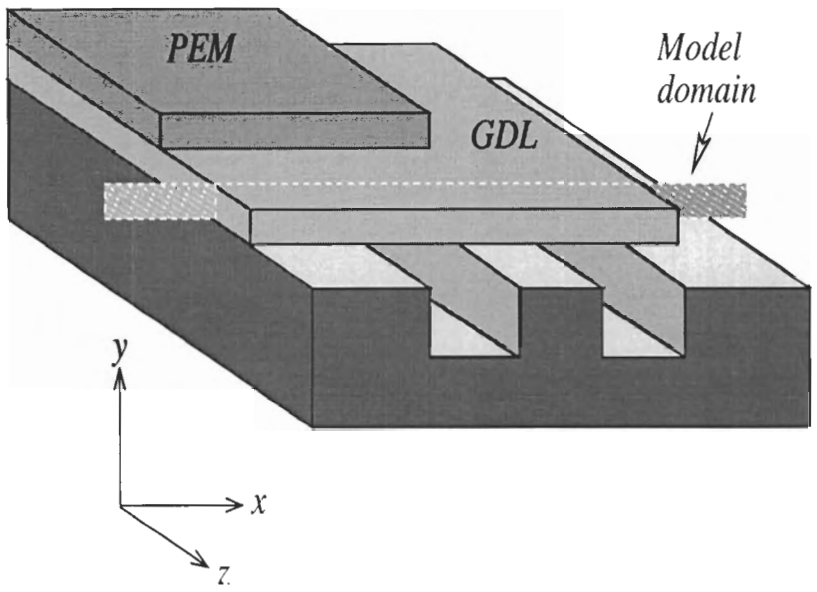

Figure 2.1: A 3D view of the PEM fuel cell (from [23]). In the model, we take a slice in the y-direction through the GDL from the channel to the PEM.

- which is standard for carbon fiber paper. This void fraction will be occupied by both gas and liquid. The fraction occupied by liquid water we will call β. The remaining fraction, occupied by gas, will then be $1-\beta$. As well, we will let the GDL equations be independent of the other components in the fuel cell and couple them via the appropriate boundary conditions.

Within the GDL, the three principle gases are the reactant gases, hydrogen and oxygen, and the inert gas, nitrogen. We will only include these three gases within the model. So the total molar gas concentration, C, is a sum of the three molar concentrations. We will call $\hat{C}_1$ the molar concentration of O_2, $\hat{C}_2$ the molar concentration of water vapour and $\hat{C}_3$ the molar concentration of nitrogen. We do not explicitly solve for the nitrogen molar concentration in this model, but we do solve for the total gas concentration, $\hat{C}$, where:

$$\hat{C} = \hat{C}_1 + \hat{C}_2 + \hat{C}_3 \tag{2.1}$$

We will also let ρ_k and M_k (k=1,2,3) denote the densities and molar masses of

oxygen, water vapour and nitrogen respectively. Where:

$$\rho = \Sigma_k \rho_k \tag{2.2}$$

and

$$M_k = \frac{\rho_k}{\hat{C}_k} \tag{2.3}$$

2.1 The Conservation Equations for the Reactant Gases

In the model, we will describe the variations in the oxygen, water vapour, and total gas molar concentrations as well as the liquid water volume fraction and temperature all in the y-direction. The first four quantities will be given by conservation equations, the fifth, temperature, will be given by an energy equation. Each of these equations is based upon a model created by Promislow, Stockie and Wetton [23].

The total volume fraction occupied by the total gas is $1 - \beta$, as noted earlier. Let us now define α as follows:

$$\alpha = (1 - \beta)$$

The mass per volume of this gas is given by $(1 - \beta)\rho$. During the operation of the fuel cell it can be described by the following conservation equation [23]:

$$\frac{\partial}{\partial \hat{t}}[\alpha\rho] + \bigtriangledown \cdot (\rho U_g) = -M\hat{\Gamma} \tag{2.4}$$

The second term U_g is the mass-averaged gas velocity and ρU_g is the mass flux of the gas in the GDL. The third term, $\hat{\Gamma}$ is the rate of condensation/evaporation due to over/under saturation. Both of these terms will be described later on. The equation can be modified with the following definition [23]:

$$\alpha = 1 - \beta \qquad \rho = M\hat{C} \tag{2.5}$$

then (2.4) becomes:

$$\begin{aligned} \frac{\partial}{\partial t}(\alpha M\hat{C}) + \bigtriangledown \cdot (M\hat{C}U_g) &= -M\hat{\Gamma} \\ \frac{\partial}{\partial t}(\alpha\hat{C}) + \bigtriangledown \cdot (\hat{C}U_g) &= -\hat{\Gamma} \end{aligned}$$

The oxygen and water vapour equations are, like the total gas molar concentration equation, both conservation of mass equations. The one major difference between the equations is that the total gas flux is only driven by convection, whereas the oxygen and water vapour fluxes are also driven by diffusion. Their fluxes are given by the following equation [23]:

$$N_k = \hat{C}_k U_g + J_k \tag{2.6}$$

where J_k is the molar diffusive flux (relative to the mass-averaged velocity) of the k^{th} species and can be given by the following formula (to be derived in the next section):

$$J_k = D\hat{C}\left[\frac{\hat{C}_k}{\hat{C}}\right]_{\hat{y}} \tag{2.7}$$

From (2.7) we can see that there is no diffusive flux for the total gas concentration:

$$\begin{aligned} J_1 + J_2 + J_3 &= D\hat{C}\left[\frac{\hat{C}_1 + \hat{C}_2 + \hat{C}_3}{\hat{C}}\right]_{\hat{y}} \\ &= D\hat{C}\left[\frac{\hat{C}}{\hat{C}}\right]_{\hat{y}} \\ &= 0 \end{aligned}$$

Let us now write the molar concentration equations for oxygen and water vapour as follows [23]:

$$\frac{\partial}{\partial \hat{t}}[\alpha \hat{C}_1] + \bigtriangledown \cdot (\hat{C}_1 U_g + J_1) = 0 \tag{2.8}$$

$$\frac{\partial}{\partial \hat{t}}[\alpha \hat{C}_2] + \bigtriangledown \cdot (\hat{C}_2 U_g + J_2) = -\hat{\Gamma} \tag{2.9}$$

In (2.9) the right-hand term $\hat{\Gamma}$ is a sink-term for the water vapour lost due to condensation. In our model, we assume that the water vapour is at saturation up to leading order. Therefore (2.9) gives us a second equation to solve for $\hat{\Gamma}$ up to leading order.

2.2 Defining U_g, J_k, $\hat{\Gamma}$, P_2^{sat} and $\hat{C}_2^{sat}$

Let us assume the the gas velocity obeys Darcy's law for flow in porous media (as assumed in [23]). Then

$$U_g = -\frac{Kk_{rg}(\beta)}{\mu_g} \bigtriangledown P_g \tag{2.10}$$

Here P_g denotes the gas pressure, K denotes the permeability of the porous GDL, and μ_g denotes the gas viscosity. $k_{rg}(\beta)$ is a term added into Darcy's law to represent the relative permeability of the porous GDL to the gas phase. We will assume that the gas pressure obeys the ideal gas law:

$$P_g = \hat{C}R\hat{T} \tag{2.11}$$

where R is the universal gas constant and $\hat{T}$ is the temperature of the mixed oxygen, water vapour and nitrogen gases. We will let $k_{rg}(\beta)$ be a polynomial fit to experimental results:

$$k_{rg}(\beta) = (1-\beta)^3 \tag{2.12}$$

Defining J_k is somewhat more complicated. We will first examine the Maxwell-Stefan equations for the mole-averaged velocity J_k^* - these are the appropriate equations to use:

$$\begin{bmatrix} J_1^* \\ J_2^* \end{bmatrix} = -\hat{C}\mathbb{D}^{eff} \cdot \begin{bmatrix} \bigtriangledown(\hat{C}_1/\hat{C}) \\ \bigtriangledown(\hat{C}_2/\hat{C}) \end{bmatrix} \tag{2.13}$$

The mole-averaged velocities J_k^* (k=1,2) can be converted to mass-averaged velocities by the 2×2 conversion matrix $\mathbb{S}$ which is given as follows:

$$S_{kg} = \delta_{kj} - \frac{\hat{C}_k M_j}{\rho_g}\left(1 - \frac{M_3}{M_j}\right) \quad and \quad \begin{bmatrix} J_1 \\ J_2 \end{bmatrix} = \mathbb{S}\begin{bmatrix} J_1^* \\ J_2^* \end{bmatrix} \tag{2.14}$$

The effective diffusivity, $\mathbb{D}^{eff}$, is a 2×2 matrix as well, given by the following formula:

$$\mathbb{D}^{eff} = [\epsilon(1-\beta)^3]^{3/2}\mathbb{D} \tag{2.15}$$

where D is a 2×2 matrix of the Maxwell-Stefan diffusivities:

$$\mathbb{D} = \begin{bmatrix} D_{11} & D_{12} \\ D_{21} & D_{22} \end{bmatrix} \tag{2.16}$$

The entries D_{kj} of D are free-space diffusion coefficients that are dependent on the species concentrations and the binary gas diffusivities. While (2.15) is a Bruggeman correction and is derived from the fact that gas diffusion is inhibited by the presence of water in the GDL pores.

As now seen, the Maxwell-Stefan equation are complicated. We will simplify down the model and use Fick's Law instead - as outlined in Sec 2.1.

Let us define the rate of condensation $\hat{\Gamma}$. This rate is given by Fowler [11] who is describing annular, two-phase flows (where the degree of water oversaturation is proportional to the condensation rate $\hat{\Gamma}$),

$$\hat{\Gamma} = \begin{cases} H_o^+(1-\beta)(\hat{C}_2 - \hat{C}_2^{sat}(T)) & \text{if } \hat{C}_2 \geq \hat{C}_2^{sat}(T) \\ H_o^-\beta(\hat{C}_2 - \hat{C}_2^{sat}(T)) & \text{if } \hat{C}_2 < \hat{C}_2^{sat}(T) \end{cases}$$

This condensation rate equation also accounts for the fact that no condensation will occur once all the water is in liquid form and no evaporation will occur if all the water is in vapour form.

We will simplify down the expression for $\hat{\Gamma}$ be assuming that $0 < \beta < 1$ and consequently neglect $(1-\beta)$ and β (since we do not need to account for whether all the water is in liquid form or all the water is in vapour form). As well, we will assume that $H_0^- = H_0^+$ and define that value as $H_\pm$. Then $\hat{\Gamma}$ reduces to:

$$\hat{\Gamma} = H_\pm \left(\hat{C}_2 - \hat{C}_2^{sat}\right) \tag{2.17}$$

Finally, we will define the functions that state the pressure and concentration of the water vapour at saturation and illustrate them in Fig.2.1,

$$\begin{aligned} P_u &= 1.01325 \times 10^6 \ erg/cm^3 \\ P_2^{sat}(\hat{T}) &= P_{convert} e^{-2.18+0.029(\hat{T}-273.2)-9.18\times10^{-5}(\hat{T}-273.2)^2+1.44\times10^{-7}(\hat{T}-273.2)^3}, \quad (2.18) \\ \hat{C}_2^{sat}(\hat{T}) &= \frac{P_2^{sat}(\hat{T})}{R\hat{T}}. \quad (2.19) \end{aligned}$$

2.3 The Liquid Water Conservation Equation

Just as we used conservation of mass equations for the gas equations, we will use the same principle for the liquid water equation. In this case, the liquid water molar

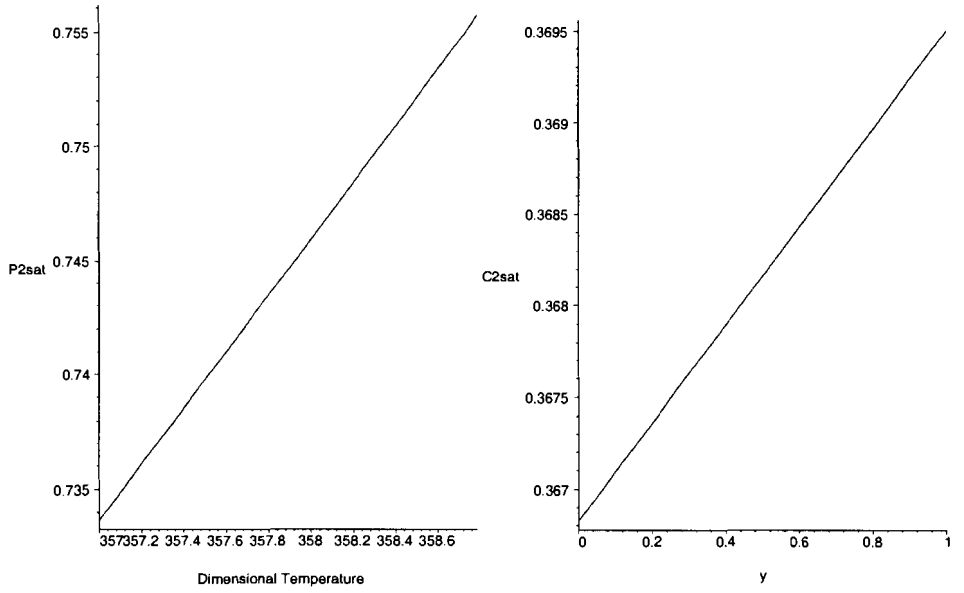

Figure 2.2: The saturation pressure, $P_2^{sat}(\hat{T})$ (left) and the saturation concentration, $C_2^{sat}(\hat{T})$ (right). $P_2^{sat}(\hat{T})$ is given in atmospheres whereas $C_2^{sat}(\hat{T})$ is given in the dimensionless form $\frac{C_2^{sat}}{\bar{C}}$ (see Chapter 3).

concentration per volume $C_l\beta$ is conserved (C_l is the liquid water concentration which is equal to ρ_l/M_2),

$$\frac{\partial}{\partial \hat{t}}(C_l\beta) + \bigtriangledown \cdot (C_l\beta U_l) = \hat{\Gamma} \tag{2.20}$$

where $\hat{\Gamma}$ is a source term for this equation (water is produced due to condensation) and the water flux is given by:

$$N_\beta = C_l\beta U_l \tag{2.21}$$

The liquid water velocity, U_l obeys Darcy's law,

$$U_l = -\frac{K k_{rl}(\beta)}{\mu_l} \bigtriangledown P_l \tag{2.22}$$

where P_l is the liquid pressure (to be defined below), μ_l is the liquid viscosity and $k_{rl}(\beta)$ is the relative liquid permeability of the GDL defined as follows,

$$k_{rl} = \begin{cases} 0 & \text{if } \beta < \beta_* \\ \frac{\sqrt{\beta-\beta_*}}{\sqrt{1-\beta_*}} & \text{if } \beta \geq \beta_* \end{cases} \tag{2.23}$$

where $k_{rl}(\beta)$ captures the hydrophobicity of the GDL, which prevents flow of liquid water if $\beta < \beta_*$.

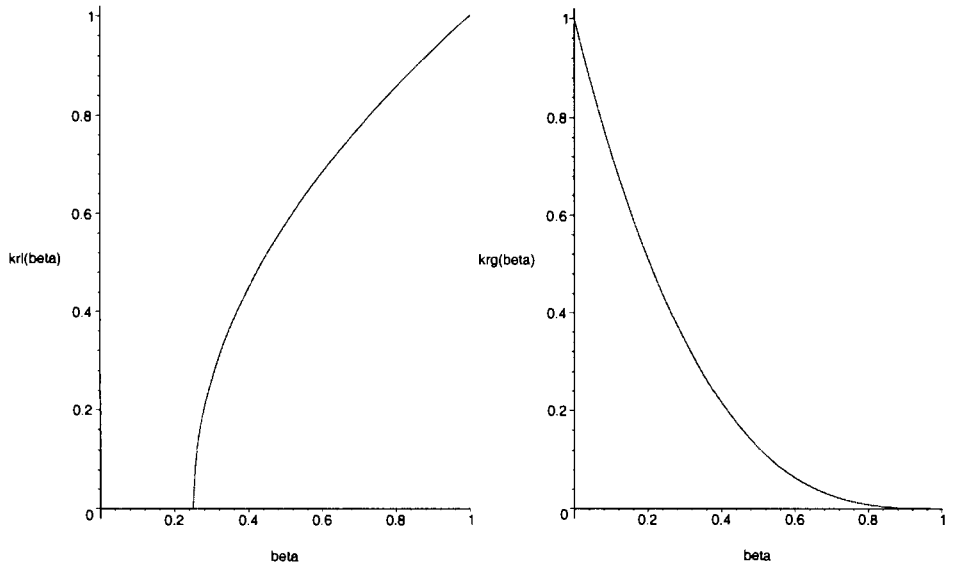

Figure 2.3: The relative liquid and gas permeabilities, $k_{rl}(\beta)$ (left) and $k_{rg}(\beta)$ (right), where the liquid water volume fraction β is varied from 0 to 1.

The liquid pressure (P_l) is due to both the capillary pressure (P_c) and the gas pressure (P_g),

$$P_l = P_g + P_c \tag{2.24}$$

where the capillary pressure is given by the following equation [23],

$$P_c = S_p \gamma_s cos(\theta) \left(\frac{\epsilon}{K}\right)^{1/2} \mathcal{J}(\beta) \tag{2.25}$$

where γ is the liquid surface tension constant, $S_p = 100$ is a scaling term in order for our capillary pressure equation to be of the right order of magnitude, θ is the contact angle between the liquid and solid phases (which is acute if the solid phase is hydrophilic and obtuse if the solid phase is hydrophobic) and $\mathcal{J}(\beta)$ is the capillary function that relates the water volume fraction quantity to the capillary pressure (the more water present, the higher the capillary pressure). For our model, let us assume

that $\theta = \frac{3\pi}{2}$ so that $cos(\theta) = -1$. Let us also define a function for $\mathcal{J}(\beta)$ that roughly fits the van Genutchen equation,

$$\mathcal{J}(\beta) = \sqrt{\frac{1}{(1-\beta)^2} - 1} \tag{2.26}$$

where the van Genutchen equation [35] is given as

$$\mathcal{J}_v(\beta) = \begin{cases} b\left[(1-\beta)^{-1/a_2} - 1\right]^{1/a_1} & \text{if } 0 < \beta \leq 1 \\ 0 & \text{otherwise} \end{cases} \tag{2.27}$$

and $a_1 = 2$, $a_2 = 1 - \frac{1}{a_1} = \frac{1}{2}$ and $b = 1$

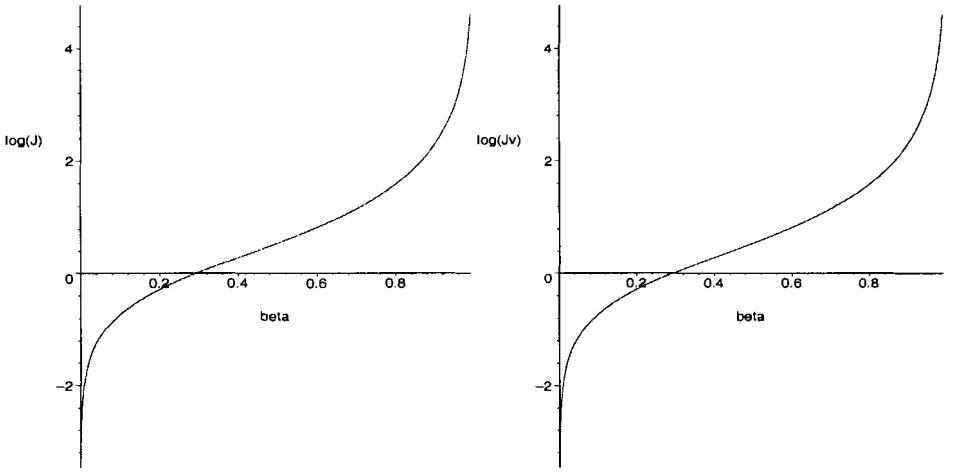

Figure 2.4: The log plots of the Leverett and van Genuchten functions, $\mathcal{J}(\beta)$ (left) and $\mathcal{J}_v(\beta)$ (right), where the liquid water volume fraction varies from 0 to 1.

2.4 The Temperature Energy Equation

We assume that the temperature is uniform amongst the three phase (since the GDL pores are so small $\approx 1\mu m$ wide) and denote it by $\hat{T}$. The energy equation is

$$\frac{\partial}{\partial t}(\tilde{\rho}c\hat{T}) + \bigtriangledown \cdot (\widetilde{\rho c U}\hat{T} - \tilde{\kappa} \bigtriangledown \hat{T}) = \frac{\overline{I}^2}{\sigma} + h_v\hat{\Gamma} \tag{2.28}$$

where c is the specific heat, $\tilde{\kappa}$ is the thermal conductivity averaged over the three phases,

$$\tilde{\kappa} = (1-\epsilon)\kappa_s + \epsilon(1-\beta)\kappa_g + \epsilon\beta\kappa_l \tag{2.29}$$

and $\widetilde{\rho c}$ and $\widetilde{\rho c U}$ are averaged over the gas and liquid phases,

$$\widetilde{\rho c} = \alpha\rho_g c_g + \beta\rho_l c_l \tag{2.30}$$

$$\widetilde{\rho c U} = \alpha\rho_g c_g U_g + \beta\rho_l c_l U_l \tag{2.31}$$

In our model, since the current is constant, $\overline{I} = I$ (where $\overline{I}$ is the average current density). σ is the electrical conductivity in the GDL and therefore the first source term is due to ohmic heating (from resistance to electron transport in the GDL). Since this term is very small, we can neglect it in our model. The second source term $h_\nu\hat{\Gamma}$ is due to the heat released by water evaporation. Through non-dimensionalization, we also see later that this term is neglible and can be ignored when solving T up to leading order.

2.5 The Boundary Conditions

2.5.1 At the channel

We assume that the gas concentrations are held fixed on the boundary of the channel and the GDL,

$$\begin{aligned}\hat{C}_1(0) &= C_1^0,\\ \hat{C}_2(0) &= C_2^0,\\ \hat{C}(0) &= \overline{C}.\end{aligned}$$

We assume that the average gas pressure is held fixed at 2 atmospheres at the channel. Then from the ideal gas law, we can find $\overline{C} = \frac{2}{R\hat{T}}$. Let us also assume that the oxygen concentration is 20 percent of the total gas concentration at the channel and that the water vapour is at saturation at the channel,

$$C_1^0 = 0.2\overline{C} \tag{2.32}$$

$$C_2^0 = \hat{C}_2^{sat}(\hat{T}(0)) \tag{2.33}$$

We prescribe the temperature to be fixed at 357^oK at the channel,

$$\hat{T}(0) = 357 \tag{2.34}$$

Unlike the gas and temperature, the liquid water volume fraction will not be held constant at the channel. We will prescribe the following boundary condition on β:

$$N_\beta = -\frac{Kk_{rg}(\beta)}{L_p\mu_l} \bigtriangledown P_l \tag{2.35}$$

This boundary condition assumes that the liquid water flux at the channel is driven by the pressure gradient. This pressure gradient is approximated by a finite difference,

$$\bigtriangledown P_l \approx \frac{0 - P_c}{L_p}$$

where L_p is the pore length, where N_β is the liquid water flux and P_c is the capillary pressure. The expression for $\bigtriangledown P_l$ and (2.35) give the boundary condition, rewritten as follows:

$$N_\beta = \frac{Kk_{rg}(\beta)}{L_p\mu_l} P_c \tag{2.36}$$

2.5.2 At the Catalyst Layer

The oxygen flux at the catalyst layer is proportional to the current I,

$$N_{\hat{C}_1} = \frac{I}{4F} \tag{2.37}$$

where $N_{\hat{C}_1}$ denotes the oxygen flux.

The water vapour flux has a similar relation to the current,

$$N_{\hat{C}_2} = -\frac{(1+\nu)I}{2F} \tag{2.38}$$

where ν denotes the negative of the percentage of water production at the catalyst layer which is in liquid form. If $\nu = 0$, then the product water is being released from the proton exchange membrane as vapour and if $\nu = -1$, all the water produced in the reaction is released as liquid water. In the case where $\nu < -1$, then liquid water is produced at a rate above the reaction by condensation. In our case, we solve for

ν from the boundary condition (2.38) and the assumption that the water vapour is at saturation up to leading order. This amounts to neglecting an $O\left(\frac{1}{H}\right)$ boundary layer. We are implicitly assuming that the product water goes into the GDL, that the membrane is saturated.

In order to obtain the total gas molar concentration boundary condition, we take a no flux condition for Nitrogen,

$$N_{C_3} = 0 \tag{2.39}$$

. This is consistent with the fact that the membrane is impermeable to gas.

Summing up the oxygen, water vapour and nitrogen concentration boundary conditions gives us the boundary condition for the total gas,

$$\begin{aligned} N_C = N_{C_1} + N_{C_2} + N_{C_3} &= \frac{I}{4F} - \frac{(1+\nu)I}{2F} \\ &= -\frac{(1+2\nu)I}{4F} \end{aligned} \tag{2.40}$$

Like the gas concentration, the liquid water volume fraction boundary condition states that the liquid water flux is proportional to the current:

$$N_\beta = \frac{\nu I}{2FC_l} \tag{2.41}$$

Finally, let us also assume that the temperature flux is proportional to the current:

$$N_T = -\frac{h_r I}{2F} + \frac{h_v I}{2F}\nu \tag{2.42}$$

where h_r denotes the heat of reaction and h_v denotes the heat of vaporization and h_r is defined as follows,

$$h_r = T \triangle S + 2F\eta_c \tag{2.43}$$

where we take a prescribed value for the cathode overpotential.

Chapter 3

The Non-Dimensional Equations

Let us choose the following new variables to render the equations dimensionless:

The Dimensionless Variables	
Time	$t = \frac{1}{t_*}\hat{t}$
Oxygen Concentration	$C_1(y) = \frac{1}{\overline{C}}\hat{C}_1$
Water Vapour Concentration	$C_2(y) = \frac{1}{\overline{C}}\hat{C}_2$
Saturation Concentration	$C_2^{sat}(y) = \frac{1}{\overline{C}}\hat{C}_2^{sat}$
Total Gas Concentration	$C(y) = \frac{1}{\overline{C}}\hat{C}$
Temperature	$T(y) = \frac{1}{T_*}\hat{T}$
GDL Thickness	$y = \frac{1}{L}\hat{y}$

Where $\overline{C} = \frac{2\times 1.01325\times 10^6}{RT_*}$, $t_* = \frac{L^2}{D} \approx 3.125 \times 10^{-2}$ and $T_* = 357$.

3.1 The oxygen equation

We start with the oxygen DE (2.8)

$$(\alpha\hat{C}_1)_{\hat{t}} + (\hat{C}_1 U_g + J_1)_{\hat{y}} = 0$$

Now, plug in the new dimensionless variables and the expressions for U_g and J_1:

$$\frac{1}{t_*}(\alpha\overline{C}C_1)_t + \frac{1}{L}\left(-\frac{\overline{C}C_1 K k_{rg}(\beta)}{L\mu_g}\left[\overline{C}RT_*T\right]_y - \frac{D\overline{C}C}{L}\left[\frac{C_1}{C}\right]_y\right)_y = 0 \qquad (3.1)$$

Multiplying through by t_* and dividing through by $\overline{C}$ and finally grouping the constant terms (including bringing the factors of D and L out of the two expressions on the right) gives:

$$(\alpha C_1)_t - \frac{t_* D}{L^2}\left(\frac{K\overline{C}RT_*}{D\mu_g}k_{rg}(\beta)C_1[CT]_y + C\left[\frac{C_1}{C}\right]_y\right)_y = 0$$

Since we know that $t_* = \frac{L^2}{D}$, this simplifies down the oxygen equation. Let us also define the following constant R_g as follows to further simplify the equation:

$$R_g = \frac{K\overline{C}RT_*}{D\mu_g}$$

Finally, with these simplifications, the oxygen equation reduces to:

$$(\alpha C_1)_t - \left(R_g k_{rg}(\beta)C_1[CT]_y + C\left[\frac{C_1}{C}\right]_y\right)_y = 0$$

3.2 The Water Vapour Equation

Let us start with the water vapour DE (2.9)

$$(\alpha\hat{C}_2)_{\hat{t}} + (\hat{C}_2 U_g + J_2)_{\hat{y}} = -\hat{\Gamma}$$

Now, again, plug in the new variables and the expressions for U_g and J_2:

$$\frac{1}{t_*}(\alpha\overline{C}C_2)_t + \frac{1}{L}\left(-\frac{\overline{C}C_2 K k_{rg}(\beta)}{L\mu_g}\left[\overline{C}RT_*T\right]_y - \frac{D\overline{C}C}{L}\left[\frac{C_2}{C}\right]_y\right)_y = -\hat{\Gamma} \tag{3.2}$$

Again, we multiply by t_* and divide by $\overline{C}$ and group the constant terms, which gives:

$$(\alpha C_2)_t - \frac{t_* D}{L^2}\left(\frac{K\overline{C}RT_*}{D\mu_g}k_{rg}(\beta)C_2[CT]_y + C\left[\frac{C_2}{C}\right]_y\right)_y = -\frac{t_*\hat{\Gamma}}{\overline{C}}$$

Again $t_* = \frac{L^2}{D}$ simplifies the equation and let us also define Γ as follows:

$$\Gamma = \frac{t_*}{\overline{C}}\hat{\Gamma}$$

Where, plugging in the definition of $\hat{\Gamma}$ (2.17) and the non-dimensional expressions for C and C_2^{sat} gives:

$$\Gamma = \frac{t_*}{\overline{C}} H_{\pm}(\overline{C}C_2 - \overline{C}C_2^{sat})$$

Canceling out $\overline{C}$ gives:

$$\Gamma = t_* H_{\pm}(C_2 - C_2^{sat})$$

Finally, let us define the new constant H:

$$H = t_* H_{\pm} \tag{3.3}$$

then Γ reduces down to the following:

$$\Gamma = H(C_2 - C_2^{sat}) \tag{3.4}$$

Finally, with these simplifications, the water vapour equation reduces to:

$$(\alpha C_2)_t - \left(R_g k_{rg}(\beta) C_2 [CT]_y + C \left[\frac{C_2}{C} \right]_y \right)_y = -\Gamma$$

3.3 The Total Gas Equation

The initial total gas DE (2.4) gives:

$$(\alpha \hat{C})_{\hat{t}} + \left(\hat{C} U_g \right)_{\hat{y}} = -\hat{\Gamma}$$

Again, we plug in the expression for U_g and the dimensionless variables:

$$\frac{1}{t_*}(\alpha \overline{C} C)_t - \frac{1}{L} \left(\overline{C} C \frac{K k_{rg}(\beta)}{L \mu_g} [\overline{C} C R T_* T]_y \right)_y = -\hat{\Gamma} \tag{3.5}$$

Dividing through by $\overline{C}$, multiplying through by t_* and grouping the constant terms again gives:

$$(\alpha C)_t - \frac{t_* D}{L^2} \left(\frac{K \overline{C} R T_*}{D \mu_g} k_{rg}(\beta) C [CT]_y \right)_y = -\frac{t_* \hat{\Gamma}}{\overline{C}}$$

By the same reasoning as the oxygen and water vapour equations we get:

$$(\alpha C)_t - (R_g k_{rg}(\beta) C [CT]_y)_y = -\Gamma$$

3.4 The Liquid Water Equation

The liquid water DE (2.20) gives:

$$\beta_{\hat{t}} + (\beta U_l)_{\hat{y}} = \frac{\hat{\Gamma}}{C_l}$$

Plugging in the dimensionless variables and the expression for U_l into the liquid water equation gives:

$$\frac{1}{t_*}\beta_t - \frac{1}{L}\left(\frac{Kk_{rl}(\beta)\beta}{L\mu_l}[\overline{C}CRT_*T]_y + \frac{KS_p\gamma_s}{L\mu_l}\left(\frac{\epsilon}{K}\right)^{1/2} k_{rl}(\beta)\beta[\mathcal{J}(\beta)]_y\right)_y = \frac{\hat{\Gamma}}{C_l} \quad (3.6)$$

Let us again multiply through by t_*, multiply and divide through by D in the right-hand term and group the constant terms:

$$\beta_t - \frac{t_*D}{L^2}\left(\frac{K\overline{C}RT_*}{D\mu_l}k_{rl}(\beta)\beta[CT]_y + \frac{KS_p\gamma_s}{D\mu_l}\left(\frac{\epsilon}{K}\right)^{1/2} k_{rl}(\beta)\beta\mathcal{J}'(\beta)\beta_y\right)_y = \frac{\overline{C}}{C_l}\frac{t_*\hat{\Gamma}}{\overline{C}}$$

Finally let us define the following two constants to simplify the liquid water equation:

$$\delta_l = \frac{\overline{C}}{C_l}$$

$$R_c = \frac{KS_p\gamma_s}{D\mu_l}\left(\frac{\epsilon}{K}\right)^{1/2}$$

Plugging these simplifications and R_g and Γ into the liquid water equation gives:

$$\beta_t - (R_l\beta k_{rl}(\beta)[CT]_y + R_c\beta k_{rl}(\beta)\mathcal{J}'(\beta)\beta_y)_y = \delta_l\Gamma$$

3.5 The Temperature Equation

Let us start with the dimensional temperature DE (2.28):

$$\left(\widetilde{\rho c}\hat{T}\right)_{\hat{t}} + \left(\widetilde{\rho cU}\hat{T} - \tilde{\kappa}\hat{T}_{\hat{y}}\right)_{\hat{y}} = h_v\hat{\Gamma} + \frac{\overline{I}^2}{\sigma}$$

We know that

$$\widetilde{\rho cU} = \alpha\rho_g c_g U_g + \beta\rho_l c_l U_l$$

Plugging in the expressions for U_g and U_l into $\widetilde{\rho c U}$ gives:

$$\widetilde{\rho c U} = -\alpha\rho_g c_g \frac{K k_{rg}(\beta)}{\mu_g}\left[\hat{C}R\hat{T}\right]_{\hat{y}} - \beta\rho_l c_l \frac{K k_{rl}(\beta)}{\mu_l}\left[\hat{C}R\hat{T} + S_p\gamma_s\left(\frac{\epsilon}{K}\right)^{1/2}\mathcal{J}(\beta)\right]_{\hat{y}} \quad (3.7)$$

Now, if we plug in (3.7) into (??), we get:

$$\begin{aligned}\left(\widetilde{\rho c}\hat{T}\right)_{\hat{t}} + (-\alpha\rho_g c_g \frac{K k_{rg}(\beta)}{\mu_g}\hat{T}\left[\hat{C}R\hat{T}\right]_{\hat{y}} - \beta\rho_l c_l \frac{K k_{rl}(\beta)}{\mu_l}\hat{T}\left[\hat{C}R\hat{T}\right]_{\hat{y}} \quad (3.8)\\ - \beta\rho_l c_l \frac{K k_{rl}(\beta)}{\mu_l}\hat{T}\left[S_p\gamma_s\left(\frac{\epsilon}{K}\right)^{1/2}\mathcal{J}(\beta)\right]_{\hat{y}} - \tilde{\kappa}\hat{T}_{\hat{y}})_{\hat{y}} \quad = \quad h_v\hat{\Gamma} + \frac{\overline{I}^2}{\sigma}\end{aligned}$$

Substituting in the dimensionless variables:

$$\begin{aligned}\frac{1}{t_*}(\widetilde{\rho c}T_*T)_t + \frac{1}{L}(-\alpha\rho_g c_g \frac{K k_{rg}(\beta)}{\mu_g L}T_*T\left[\overline{C}CRT_*T\right]_y - \beta\rho_l c_l \frac{K k_{rl}(\beta)}{\mu_l L}T_*T\left[\overline{C}CRT_*T\right]_y\\ - \beta\rho_l c_l \frac{K k_{rl}(\beta)}{\mu_l L}T_*T\left[S_p\gamma_s\left(\frac{\epsilon}{K}\right)^{1/2}\mathcal{J}(\beta)\right]_y - \frac{\tilde{\kappa}}{L}T_*T_y)_y \quad = \quad h_v\hat{\Gamma} + \frac{\overline{I}^2}{\sigma} \quad (3.9)\end{aligned}$$

Now, we multiply through by t_* and divide by T_*:

$$\begin{aligned}\widetilde{\rho c}T_t + \frac{t_*}{L}(-\alpha\rho_g c_g \frac{K k_{rg}(\beta)}{\mu_g L}T\left[\overline{C}CRT_*T\right]_y - \beta\rho_l c_l \frac{K k_{rl}(\beta)}{\mu_l L}T\left[\overline{C}CRT_*T\right]_y\\ - \beta\rho_l c_l \frac{K k_{rl}(\beta)}{\mu_l L}T\left[S_p\gamma_s\left(\frac{\epsilon}{K}\right)^{1/2}\mathcal{J}(\beta)\right]_y - \frac{\tilde{\kappa}}{L}T_y)_y \quad = \quad \frac{h_v t_*}{T_*}\hat{\Gamma} + \frac{t_*}{T_*}\frac{\overline{I}^2}{\sigma} \quad (3.10)\end{aligned}$$

Let us assume that α and β are roughly constant. So $\alpha \approx \alpha_*$ and $\beta \approx \beta_*$, where $\alpha_* = 0.75$ and $\beta_* = 0.25$. Let us approximate $\widetilde{\rho c}$ by:

$$\widetilde{\rho c} = \alpha_*\rho_g c_g + \beta_*\rho_l c_l \quad (3.11)$$

Treating $\widetilde{\rho c}$ as a constant value allows us to divide it out of the t and y derivative terms on the left-hand side of the temperature equation.

$$\begin{aligned}T_t + \frac{t_*}{L}(-\alpha\rho_g c_g \frac{K k_{rg}(\beta)}{\widetilde{\rho c}\mu_g L}T\left[\overline{C}CRT_*T\right]_y - \beta\rho_l c_l \frac{K k_{rl}(\beta)}{\widetilde{\rho c}\mu_l L}T\left[\overline{C}CRT_*T\right]_y\\ - \beta\rho_l c_l \frac{K k_{rl}(\beta)}{\widetilde{\rho c}\mu_l L}T\left[S_p\gamma_s\left(\frac{\epsilon}{K}\right)^{1/2}\mathcal{J}(\beta)\right]_y - \frac{\tilde{\kappa}}{\widetilde{\rho c}L}T_y)_y \quad = \quad \frac{h_v t_*}{\widetilde{\rho c}T_*}\hat{\Gamma} + \frac{t_*}{\widetilde{\rho c}T_*}\frac{\overline{I}^2}{\sigma} \quad (3.12)\end{aligned}$$

Finally, let us group all the constant terms together and multiply and divide by D in the convection and diffusion terms and by $\overline{C}$ on the right-hand side:

$$T_t - \frac{t_* D}{L^2}(\left(\frac{\rho_g c_g}{\widetilde{\rho c}}\right)\left(\frac{K\overline{C}RT_*}{D\mu_g}\right)\alpha k_{rg}(\beta)T[CT]_y + \left(\frac{\rho_l c_l}{\widetilde{\rho c}}\right)\left(\frac{K\overline{C}RT_*}{D\mu_l}\right)\beta k_{rl}(\beta)T[CT]_y$$
$$+\left(\frac{\rho_l c_l}{\widetilde{\rho c}}\right)\left(\frac{KS_p\gamma_s}{D\mu_l}\left(\frac{\epsilon}{K}\right)^{1/2}\right)\beta k_{rl}(\beta)\mathcal{J}'(\beta)\beta_y T + \left(\frac{\tilde{\kappa}}{D\widetilde{\rho c}}\right)T_y)_y = \left(\frac{h_v\overline{C}}{\widetilde{\rho c}T_*}\right)\frac{t_*\hat{\Gamma}}{\overline{C}} + \frac{t_*}{\widetilde{\rho c}}$$

Let us now name the following constants to reduce down the temperature equation:

$$r_g = \left(\frac{\rho_g c_g}{\widetilde{\rho c}}\right)\left(\frac{K\overline{C}RT_*}{D\mu_g}\right) = \left(\frac{\rho_g c_g}{\widetilde{\rho c}}\right)R_g$$

$$r_l = \left(\frac{\rho_l c_l}{\widetilde{\rho c}}\right)\left(\frac{K\overline{C}RT_*}{D\mu_l}\right) = \left(\frac{\rho_l c_l}{\widetilde{\rho c}}\right)R_l$$

$$r_c = \left(\frac{\rho_l c_l}{\widetilde{\rho c}}\right)\left(\frac{KS_p\gamma_s}{D\mu_l}\left(\frac{\epsilon}{K}\right)^{1/2}\right) = \left(\frac{\rho_l c_l}{\widetilde{\rho c}}\right)R_c$$

$$F_b = \left(\frac{\tilde{\kappa}}{D\widetilde{\rho c}}\right)$$

$$\delta_T = \left(\frac{h_v\overline{C}}{\widetilde{\rho c}T_*}\right)$$

When we plug in these constants and $\Gamma = \frac{t_*\hat{\Gamma}}{\overline{C}}$, we get the following reduced temperature equation:

$$T_t - (r_g\alpha k_{rg}(\beta)T[CT]_y + r_l\beta k_{rl}(\beta)T[CT]_y + r_c\beta k_{rl}(\beta)\mathcal{J}'(\beta)\beta_y T + F_b T_y)_y = \delta_T\Gamma + \frac{t_*}{\widetilde{\rho c}T_*}\frac{\overline{I}^2}{\sigma}$$

Chapter 4

The Non-dimensional Boundary Conditions

4.1 The Oxygen Boundary Conditions

4.1.1 At the channel ($\hat{y} = 0$)

We start with the dimensional boundary condition $\hat{C}_1(0) = 0.2\overline{C}$ when we add the in dimensionless parameters we get:

$$\boxed{C_1(0) = 0.2} \tag{4.1}$$

4.1.2 At the catalyst layer

Now, take the dimensional boundary conditions at $\hat{y} = L$,

$$N_{\hat{C}_1}|_{\hat{y}=L} = \frac{I}{4F} \tag{4.2}$$

The dimensional expression for the oxygen flux is as follows:

$$N_{\hat{C}_1} = \hat{C}_1 U_g + J_1$$

We have seen the non-dimensionalization of this flux term in section 3.1, equation (3.1), and from it we can determine the following expression for the non-dimensional

oxygen flux:

$$N_{C_1} = -\frac{\overline{C}^2 KRT_*}{L\mu_g} C_1 k_{rg}(\beta)[CT]_y - \frac{D\overline{C}}{L} C \left[\frac{C_1}{C}\right]_y$$

Grouping the constants in the above expression gives:

$$N_{\hat{C}_1} = -\frac{\overline{C}D}{L}\frac{K\overline{C}RT_*}{D\mu_g} k_{rg}(\beta) C_1 [CT]_y - \frac{\overline{C}D}{L} C \left[\frac{C_1}{C}\right]_y$$

Substituting in R_g gives:

$$N_{C_1} = -\frac{\overline{C}D}{L} R_g k_{rg}(\beta) C_1 [CT]_y - \frac{\overline{C}D}{L} C \left[\frac{C_1}{C}\right]_y \tag{4.3}$$

So, the oxygen boundary condition at the GDL becomes:

$$-\frac{\overline{C}D}{L} R_g k_{rg}(\beta) C_1 [CT]_y - \frac{\overline{C}D}{L} C \left[\frac{C_1}{C}\right]_y |_{y=1} = \frac{I}{4F}$$

Dividing both sides through by $-\frac{\overline{C}D}{L}$ gives:

$$R_g k_{rg}(\beta) C_1 [CT]_y + C \left[\frac{C_1}{C}\right]_y |_{y=1} = -\frac{IL}{4F\overline{C}D}$$

Let us now define I_0 to simplify down the right hand side of the above equation:

$$I_0 = \frac{IL}{4F\overline{C}D} \tag{4.4}$$

In effect, I_0 is the oxygen consumption rate at the membrane. Plugging it into the boundary condition gives:

$$\boxed{R_g k_{rg}(\beta) C_1 [CT]_y + C \left[\frac{C_1}{C}\right]_y |_{y=1} = -I_0} \tag{4.5}$$

4.2 The Water Vapour Boundary Conditions

4.2.1 At the channel

Since we are assuming that the water vapour is at saturation up to leading order, we get the following boundary condition at the channel:

$$\hat{C}_2(0) = C_2^0 = \hat{C}_2^{sat}(T(0))$$

We can nondimensionalize this boundary condition as follows:

$$\boxed{C_2(0) = C_2^{sat}(0)} \tag{4.6}$$

4.2.2 At the catalyst layer

Assuming that the water vapour flux is proportional to the current at the GDL, we get the boundary condition,

$$N_{\hat{C}_2}|_{\hat{y}=L} = -\frac{(1+\nu)I}{2F}$$

Again, like the oxygen flux, we have non-dimensionalized the water vapour flux when we non-dimensionalized the water vapour DE in section 3.2 - equation (3.2). So, from these results, the flux can be written as follows:

$$N_{C_2} = -\frac{\overline{C}^2 KRT_*}{L\mu_g} k_{rg}(\beta) C_2 [CT]_y - \frac{D\overline{C}}{L} C \left[\frac{C_2}{C}\right]_y$$

Grouping the constant terms in the above expression gives:

$$N_{\hat{C}_2} = -\frac{\overline{C}D}{L}\frac{K\overline{C}RT_*}{D\mu_g} k_{rg}(\beta) C_2 [CT]_y - \frac{\overline{C}D}{L} C \left[\frac{\overline{C}C_2}{\overline{C}C}\right]_y$$

Substituting in R_g gives:

$$N_{C_2} = -\frac{\overline{C}D}{L} R_g k_{rg}(\beta) C_2 [CT]_y - \frac{\overline{C}D}{L} C \left[\frac{C_2}{C}\right]_y \tag{4.7}$$

Therefore, from above result, our water vapour boundary condition at the GDL can be written as:

$$-\frac{\overline{C}D}{L} R_g k_{rg}(\beta) C_2 [CT]_y - \frac{\overline{C}D}{L} C \left[\frac{C_2}{C}\right]_y |_{y=1} = -\frac{(1+\nu)I}{2F}$$

Dividing both sides through by $-\frac{\overline{C}D}{L}$ gives:

$$R_g k_{rg}(\beta) C_2 [CT]_y + C \left[\frac{C_2}{C}\right]_y |_{y=1} = \frac{(1+\nu)IL}{2F\overline{C}D} \tag{4.8}$$

The right-hand side of the above expression can be rewritten as follows:

$$\frac{(1+\nu)IL}{2F\overline{C}D} = 2(1+\nu)\frac{IL}{4F\overline{C}D}$$

Substituting in I_0 gives:

$$\frac{(1+\nu)IL}{2F\overline{C}D} = 2(1+\nu)I_0 \tag{4.9}$$

Equating the LHS of (4.8) and the RHS of (4.9) gives the following boundary condition:

$$\boxed{R_g k_{rg}(\beta)C_2[CT]_y + C\left[\frac{C_2}{C}\right]_y|_{y=1} = 2(1+\nu)I_0} \tag{4.10}$$

From this boundary condition, we notice that the water vapour flux at the membrane is $-2(1+\nu)$ times that of the oxygen flux. From this, we can determine that if $\nu = -1$, all the water vapour produced is released as liquid water.

4.3 The Total Gas Boundary Conditions

4.3.1 At the channel

As we stated earlier, the total gas concentration at the channel is as follows:

$$\hat{C}(0) = \overline{C}$$

The resulting dimensionless boundary condition (when we divide both sides by $\overline{C}$) becomes:

$$\boxed{C(0) = 1} \tag{4.11}$$

4.3.2 At the catalyst layer

Let us start with the total gas boundary condition:

$$N_{\hat{C}}|_{\hat{y}=L} = -\frac{(1+2\nu)I}{4F}$$

The total gas flux can be written in dimensionless form as follows (see section 2.3 , equation (3.5) for further details):

$$N_C = -\frac{\overline{C}^2 KRT_*}{L\mu_g}k_{rg}(\beta)C[CT]_y$$

Grouping the constant terms gives:

$$\begin{aligned} N_C &= -\frac{\overline{C}D}{L}\frac{KRT_*\overline{C}}{D\mu_g}k_{rg}(\beta)C[CT]_y \\ &= -\frac{\overline{C}D}{L}R_g k_{rg}(\beta)C[CT]_y \end{aligned} \tag{4.12}$$

Therefore, the boundary condition then becomes:

$$\frac{\overline{C}D}{L}R_g k_{rg}(\beta)C[CT]_y = \frac{(1+2\nu)I}{4F}$$

Dividing both sides through by $\frac{\overline{C}D}{L}$ gives:

$$R_g k_{rg}(\beta)C[CT]_y = \frac{(1+2\nu)IL}{4F\overline{C}D} \tag{4.13}$$

The right-hand side of the above expression can be rewritten as follows:

$$\frac{(1+2\nu)IL}{4F\overline{C}D} = (1+2\nu)\frac{IL}{4F\overline{C}D}$$

Substituting I_0 into the above expression gives:

$$\frac{(1+2\nu)IL}{4F\overline{C}D} = (1+2\nu)I_0 \tag{4.14}$$

Equating (4.13) and (4.14) gives the following boundary condition for the total gas concentration at the catalyst layer:

$$\boxed{R_g k_{rg}(\beta)C[CT]_y = (1+2\nu)I_0} \tag{4.15}$$

4.4 The Liquid Water Boundary Conditions

4.4.1 At the channel

Recall the liquid water boundary condition at the channel (2.36)

$$N_\beta = \frac{Kk_{rl}(\beta)}{L_p\mu_l}P_c$$

We have already non-dimensionalized the liquid water flux in section 3.4 - see (3.6), and N_β can be expressed as follows:

$$N_\beta = -\frac{K\overline{C}RT_*}{L\mu_l}\beta k_{rl}(\beta)[CT]_y - \frac{KS_p\gamma_s}{L\mu_l}\left(\frac{\epsilon}{K}\right)^{1/2}\beta k_{rl}(\beta)\mathcal{J}'(\beta)\beta_y$$

Grouping the constant terms gives:

$$N_\beta = -\frac{D}{L}\frac{K\overline{C}RT_*}{D\mu_l}\beta k_{rl}(\beta)[CT]_y - \frac{D}{L}\frac{KS_p\gamma_s}{D\mu_l}\left(\frac{\epsilon}{K}\right)^{1/2}\beta k_{rl}(\beta)\mathcal{J}'(\beta)\beta_y$$

Finally, substituting in R_l and R_c gives:

$$N_\beta = -\frac{D}{L}R_l\beta k_{rl}(\beta)[CT]_y - \frac{D}{L}R_c\beta k_{rl}(\beta)\mathcal{J}'(\beta)\beta_y \tag{4.16}$$

Let us now rewrite the RHS of (2.36) by substituting in the expression for P_c:

$$\frac{Kk_{rl}(\beta)}{L_p\mu_l}P_c = -\frac{Kk_{rl}(\beta)S_p\gamma_s}{L_p\mu_l}\left(\frac{\epsilon}{K}\right)^{1/2}\mathcal{J}(\beta)$$

Regrouping the constants and multiplying both the numerator and denomenator on the right-hand side by D gives:

$$\frac{Kk_{rl}(\beta)}{L_p\mu_l}P_c = -\frac{D}{L_p}\frac{KS_p\gamma_s}{D\mu_l}\left(\frac{\epsilon}{K}\right)^{1/2}k_{rl}(\beta)\mathcal{J}(\beta)$$

Finally, substituting in R_c gives:

$$\frac{Kk_{rl}(\beta)}{L_p\mu_l}P_c = -\frac{D}{L_p}R_ck_{rl}(\beta)\mathcal{J}(\beta) \tag{4.17}$$

Equating (4.17) and (4.16) gives the following boundary condition:

$$-\frac{D}{L}R_l\beta k_{rl}(\beta)[CT]_y - \frac{D}{L}R_c\beta k_{rl}(\beta)\mathcal{J}'(\beta)\beta_y = -\frac{D}{L_p}R_ck_{rl}(\beta)\mathcal{J}(\beta)$$

Dividing both sides through by $-\frac{DR_c}{L}$ gives:

$$\boxed{\frac{R_l}{R_c}\beta k_{rl}(\beta)[CT]_y + \beta k_{rl}(\beta)\mathcal{J}'(\beta)\beta_y = \frac{L}{L_p}k_{rl}(\beta)\mathcal{J}(\beta)} \tag{4.18}$$

4.4.2 At the catalyst layer

The liquid water boundary condition at the catalyst layer (2.41) is as follows:

$$N_\beta|_{\hat{y}=L} = \frac{\nu I}{2FC_l}$$

We know the expression for the water flux (4.16) from the previous section and can therefore rewrite the boundary condition at the catalyst layer as follows:

$$-\frac{D}{L}\left[R_l\beta k_{rl}(\beta)[CT]_y - R_c\beta k_{rl}(\beta)\mathcal{J}'(\beta)\beta_y\right]_{y=1} = \frac{\nu I}{2FC_l}$$

Dividing through by $-\frac{DR_c}{L}$ gives:

$$\left[\frac{R_l}{R_c}\beta k_{rl}(\beta)[CT]_y + \beta k_{rl}(\beta)\mathcal{J}'(\beta)\beta_y\right]_{y=1} = -\frac{\nu IL}{2FC_lDR_c} \tag{4.19}$$

The RHS of (4.19) can be rewritten as follows:

$$-\frac{\nu IL}{2FC_lDR_c} = -\nu\frac{2\overline{C}}{C_lR_c}\frac{IL}{4F\overline{C}D}$$

Let us define the constant θ_β:

$$\theta_\beta = \frac{2\overline{C}}{C_lR_c} \tag{4.20}$$

Substituting θ_β and I_0 into the RHS of (4.19) gives:

$$-\frac{\nu IL}{2FC_lDR_c} = -\nu\theta_\beta I_0 \tag{4.21}$$

Equating the RHS of (4.21) and the LHS of (4.19) gives the following boundary condition for the liquid water at the catalyst layer:

$$\boxed{\left[\frac{R_l}{R_c}\beta k_{rl}(\beta)[CT]_y + \beta k_{rl}(\beta)\mathcal{J}'(\beta)\beta_y\right]_{y=1} = -\nu\theta_\beta I_0} \tag{4.22}$$

This boundary condition implies that the liquid water flux is $\nu\theta_\beta$ times that of the oxygen flux at the catalyst layer. From this, we can conclude that if $\nu = 0$, all the water produced at the membrane is being released as vapour and none as liquid.

4.5 The Temperature Boundary Conditions

4.5.1 At the channel

Our boundary condition at y=0:

$$\hat{T}|_{\hat{y}=0} = T_*$$

which can be nondimensionalized as:

$$\boxed{T|_{y=0} = 1} \tag{4.23}$$

4.5.2 At the catalyst layer

Recall the temperature boundary condition at the catalyst layer (2.42):

$$N_T|_{\hat{y}=L} = -\frac{h_r I}{2F} - \frac{h_v I}{2F}\nu$$

The temperature flux, N_T was non-dimensionalized in section 3.5. From (3.9), we get the following:

$$\begin{aligned} N_T = \; & - \alpha k_{rg}(\beta)\frac{\rho_g c_g}{L}\frac{KT_*^2\overline{C}R}{\mu_g}T[CT]_y - \beta k_{rl}(\beta)\frac{\rho_l c_l}{L}\frac{KT_*^2\overline{C}R}{\mu_l}T[CT]_y \\ & - \beta k_{rl}(\beta)\frac{\rho_l c_l}{L}\frac{KT_* S_p\gamma_s}{\mu_l}\left(\frac{\epsilon}{K}\right)^{1/2}\mathcal{J}'(\beta)\beta_y - \frac{\tilde{\kappa}T_*}{L}T_y \end{aligned}$$

From the above expression, bringing out $\frac{1}{L}$, multiplying and dividing by $\widetilde{\rho c}T_*D$ gives:

$$\begin{aligned} N_T = -\frac{1}{L}\Bigg[& \frac{\rho_g c_g}{\widetilde{\rho c}}\widetilde{\rho c}T_* D\frac{K\overline{C}RT_*}{D\mu_g}\alpha k_{rg}(\beta)T[CT]_y + \frac{\rho_l c_l}{\widetilde{\rho c}}\widetilde{\rho c}T_* D\frac{KT_* R\overline{C}}{D\mu_l}\beta k_{rl}(\beta)T[CT]_y \\ & + \frac{\rho_l c_l}{\widetilde{\rho c}}\widetilde{\rho c}T_* D\frac{KS_p\gamma_s}{D\mu_l}\left(\frac{\epsilon}{K}\right)^{1/2}\beta k_{rl}(\beta)\mathcal{J}'(\beta)\beta_y + T_*\widetilde{\rho c}D\frac{\tilde{\kappa}}{D\widetilde{\rho c}}T_y\Bigg] \end{aligned}$$

Bringing out $\widetilde{\rho c}T_*D$ and substituting in r_g, r_l, r_c and F_b gives:

$$N_T = -\frac{\widetilde{\rho c}T_* D}{L}\left(r_g T[CT]_y + r_l\beta k_{rl}(\beta)T[CT]_y + r_c f(\beta)\beta_y T + F_b T_y\right)$$

From this expression, we can rewrite the boundary condition at the catalyst layer as follows:

$$\frac{\widetilde{\rho c}T_* D}{L}\left(r_g T[CT]_y + r_l\beta k_{rl}(\beta)T[CT]_y + r_c f(\beta)\beta_y T + F_b T_y\right) = \frac{(h_r - h_v\nu)I}{2F}$$

Dividing both sides by $\frac{\widetilde{\rho}\widetilde{c}T_*D}{L}$ gives:

$$r_g T[CT]_y + r_l \beta k_{rl}(\beta) T[CT]_y + r_c f(\beta)\beta_y T + F_b T_y = \frac{(h_r - h_v\nu)IL}{2F\widetilde{\rho}\widetilde{c}T_*D} \tag{4.24}$$

The RHS of (4.24) can be rewritten as follows:

$$\frac{(h_r - h_v\nu)IL}{2F\widetilde{\rho}\widetilde{c}T_*D} = \frac{2(h_r - h_v\nu)\overline{C}}{\widetilde{\rho}\widetilde{c}T_*} \frac{IL}{4F\overline{C}D} \tag{4.25}$$

We define θ_T as follows:

$$\theta_T = \frac{2\overline{C}h_r}{\widetilde{\rho}\widetilde{c}T_*} \tag{4.26}$$

Plugging this new constant and I_0 into (4.25) gives:

$$\frac{(h_r - h_v\nu)IL}{2F\widetilde{\rho}\widetilde{c}T_*D} = (1 - \frac{h_v}{h_r}\nu)\theta_T I_0$$

Equating the RHS of the above expression with the LHS of (4.24) gives the following boundary condition for the temperature at the catalyst layer:

$$\boxed{r_g T[CT]_y + r_l \beta k_{rl}(\beta) T[CT]_y + r_c f(\beta)\beta_y T + F_b T_y = (1 - \frac{h_v}{h_r}\nu)\theta_T I_0} \tag{4.27}$$

Chapter 5

The Reduced Model

Let us first summarize the assumptions that have been made so far:

- The fuel cell runs at a prescribed current $I = 1\ amp/cm^2$.
- The water vapour is almost at saturation.
- ν is to be specified by the C_2 boundary condition at $y = 1$.
- The GDL carbon fiber paper is homogeneous (ϵ is constant).
- The gas and liquid velocities obey Darcy's Law.
- The gas pressure obeys the Ideal Gas Law.
- The contact angle θ is $\frac{3\pi}{2}$.
- The temperature is uniform amongst the three phases.
- $\frac{\bar{I}^2}{\sigma}$ is small compared to $h_v\hat{\Gamma}$.
- The oxygen concentration accounts for 20% of the total gas concentration.
- $H_0^+ = H_0^-$.
- The liquid water fraction is almost constant - $\beta \approx 0.25$.

Let us now make the following approximations, simplifications and assumptions to reduce down the equations:

5.1 The Approximations and Simplifications

- $k_{rg}(\beta) \approx 1$
- $\alpha k_{rg}(\beta) \approx 1$
- $H = H_{\pm} t_*$
- $f(\beta) = \beta k_{rl}(\beta) \mathcal{J}'(\beta)$ (which is shown in the Fig. 5.1)

5.2 The Assumptions

(A1) $\frac{I_0}{C_1} \leq O(1)$ and $\left[ln\left(\frac{C_1}{C}\right)\right]_y = O(10^1)$ // (The "Moderate Current" assumption)

(A2) $C = O(1)$

(A3) $\Gamma \ll O(1)$

(A4) $H \gg 1$ which implies $H_{\pm} \gg \frac{1}{t_*} \approx 33$

(A5) $\beta > 0$ everywhere

(A6) $\delta_l \ll 1$

Note: $\beta_* = 0.25$ is the immobile water volume fraction.

Plugging in the approximations $k_{rg}(\beta) = 1$ and $\alpha k_{rg}(\beta) = 1$ and the expression for $f(\beta)$ gives the following non-dimensional equations:

$$(\alpha C_1)_t - \left(R_g C_1 [CT]_y + C \left[\frac{C_1}{C}\right]_y \right)_y = 0 \tag{5.1}$$

$$(\alpha C_2)_t - \left(R_g C_2 [CT]_y + C \left[\frac{C_2}{C}\right]_y \right)_y = -\Gamma \tag{5.2}$$

$$(\alpha C)_t - (R_g C [CT]_y)_y = -\Gamma \tag{5.3}$$

$$\beta_t - (R_l \beta k_{rl}(\beta) [CT]_y + R_c f(\beta) \beta_y)_y = \delta_l \Gamma \tag{5.4}$$

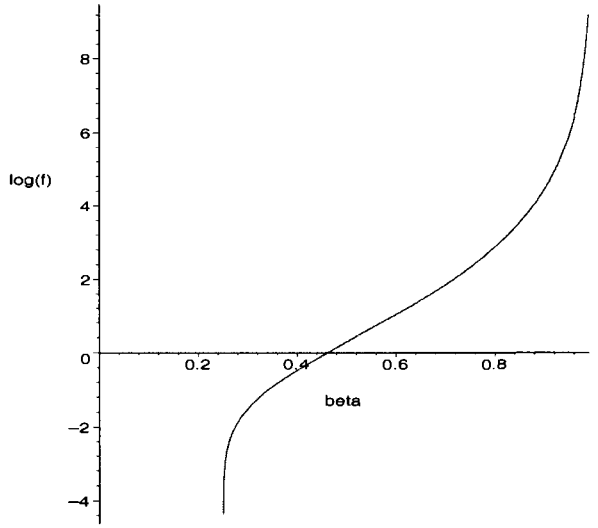

Figure 5.1: The log plot of $f(\beta) = \beta k_{rl}(\beta)\mathcal{J}'(\beta)$ for $\beta \in [0,1]$.

$$T_t - (r_g T[CT]_y + r_l \beta k_{rl}(\beta) T[CT]_y + r_c f(\beta)\beta_y T + F_b T_y)_y = \delta_T \Gamma \qquad (5.5)$$

From equations (5.1) through (5.5), we can determine the time-scales for the gases, liquid water and temperature equations. They are given in the following table:

The Time Scales		
Oxygen - $C_1(y)$	t	$O(t)$
Water vapour - $C_2(y)$	t	$O(t)$
Total gas - $C(y)$	t	$O(t)$
Liquid water - $\beta(y)$	$R_c t$	$O(t)$
Temperature - $T(y)$	$F_b t$	$O(10^1 t)$

5.3 Approximating the Size of $[CT]_y$

In order to reduce down the model, let us look at the term $[CT]_y$ since it appears in every equation. We would like to get a rough estimate of its size. We can do so by taking the oxygen equation at steady state (since steady state is what we impose

later to solve the system of equations). This equation is as follows:

$$\left(R_g C_1 [CT]_y + C\left[\frac{C_1}{C}\right]_y\right)_y = 0$$

If we integrate both sides, we get the following result (where d_1 is the constant of integration):

$$R_g k_{rg}(\beta) C_1 [CT]_y + C\left[\frac{C_1}{C}\right]_y = d_1 \tag{5.6}$$

The LHS of (5.6) can be rewritten as a flux by multiplying and dividing by $-\frac{\overline{C}D}{L}$:

$$-\frac{L}{\overline{C}D}\left(-\frac{\overline{C}D}{L} R_g k_{rg}(\beta) C_1 [CT]_y - \frac{\overline{C}D}{L} C\left[\frac{C_1}{C}\right]_y\right) = d_1$$

Now, by (4.3), the expression inside the brackets can be recognized as the oxygen flux N_{C_1}, which gives the following expression for d_1:

$$-\frac{L}{\overline{C}D} N_{C_1} = d_1$$

We can now determine d_1 from the boundary condition at the membrane (y=1) (2.37) - which gives us a value for N_{C_1}:

$$\begin{aligned} d_1 &= -\frac{L}{\overline{C}D} N_{C_1}|_{y=1} \\ &= -\frac{L}{\overline{C}D}\left(\frac{I}{4F}\right) \\ &= -I_0 \\ &\approx -2.372 \times 10^{-2} \end{aligned} \tag{5.7}$$

We will now rewrite (5.6) as an expression for $[CT]_y$:

$$[CT]_y = \frac{1}{R_g}\left(\frac{d_1}{C_1} - \frac{C}{C_1}\left[\frac{C_1}{C}\right]_y\right)$$

which can be rewritten as:

$$[CT]_y = -\frac{1}{R_g}\left(\frac{I_0}{C_1} + \left(ln\frac{C_1}{C}\right)_y\right) \tag{5.8}$$

Then apply (A1) - the Moderate Current assumption. As a result, the term inside the brackets is $O(1)$ and,

$$[CT]_y = O\left(\frac{1}{R_g}\right)$$

Since $[CT]_y$ is so small, then $R_g[CT]_y = O(1)$ and the convective and diffusive terms balance in both the oxygen and water vapour equations. As well, the time scale for C ($R_g[CT]_y$) is also roughly O(1).

5.4 Approximating the size of $P^{(1)}$

The total gas boundary condition at the catalyst layer gives:

$$[R_g C[CT]_y]_{y=1} = (1 + 2\nu)I_0 \tag{5.9}$$

As defined in the previous section (5.3),

$$R_g[CT]_y = P_y^{(1)} + O\left(\frac{1}{R_g}\right).$$

Therefore, equation (5.9) becomes:

$$C\left(P_y^{(1)} + O\left(\frac{1}{R_g}\right)\right) = (1 + 2\nu)I_0$$

By (A2), we know that $C(y) = O(1)$. Also, since $\nu = O(1)$, then $(1 + 2\nu) = O(1)$ as well. Consequently,

$$\begin{aligned} P_y^{(1)} &= O\left(I_0, \frac{1}{R_g}\right) \\ &= O(I_0) \end{aligned} \tag{5.10}$$

5.5 The constants

Given Constants					
C_l	0.0556	mol/cm^3	h_r	4.033×10^{11}	erg/mol
D	0.08	cm^2/s	κ_g	2.8×10^3	$erg/cm\ s\ ^oK$
F	96485	C/mol	κ_l	6.75×10^4	$erg/cm\ s\ ^oK$
K	10^{-8}	cm^2	κ_s	10^5	$erg/cm\ s\ ^oK$
R	8.3145×10^7	$erg/mol\ ^oK$	μ_g	2.24×10^{-4}	$g/cm\ s$
c_g	2.6×10^7	$erg/g\ ^oK$	μ_l	3	$g/cm\ s$
c_l	10^7	$erg/g\ ^oK$	ρ_g	2×10^{-3}	g/cm^3
c_s	7.1×10^6	$erg/g\ ^oK$	ρ_l	1	g/cm^3
γ_s	72.4	g/s^2	ρ_s	0.49	g/cm^3
h_v	4.54×10^{11}	erg/mol	σ	7.273×10^{-5}	$amp^2\ s/erg\ cm$
Chosen Constants					
α_*	0.75	-	S_p	100	-
β_*	0.25	-	T_*	357	^oK
$\overline{C}$	6.827×10^{-5}	mol/cm^3	$\tilde{\rho c}$	2.539×10^6	$erg/cm^3\ ^oK$
I	1	amp/cm^2	$\tilde{\kappa}$	2.614×10^6	$erg/cm\ s\ ^oK$
L	0.05	cm	ϵ	0.74	-
Constants Created by Non-Dimensionalizing					
F_b	1.971×10^{-1}	$\frac{\tilde{\kappa}}{\tilde{\rho c} D}$	δ_T	3.420×10^{-2}	$\frac{h_v \overline{C}_1}{\tilde{\rho c} T_*}$
R_c	2.595	$\frac{S_p K \gamma_s}{\mu_l D} \left(\frac{\epsilon}{K}\right)^{1/2}$	r_c	1.022×10^1	$\left(\frac{\rho_l c_l}{\tilde{\rho c}}\right) R_c$
R_g	1.130×10^3	$\frac{R T_* K \overline{C}}{D \mu_g}$	r_g	2.316×10^1	$\left(\frac{\rho_g c_g}{\tilde{\rho c}}\right) R_g$
R_l	8.444×10^{-2}	$\frac{\mu_g R_g}{\mu_l}$	r_l	3.325×10^{-1}	$\left(\frac{\rho_l c_l}{\tilde{\rho c}}\right) R_l$
δ_l	1.228×10^{-3}	$\frac{\overline{C}_1}{C_l}$	t_*	3.125×10^{-2}	$\frac{L^2}{D}$
I_0	2.372×10^{-2}	$\frac{IL}{4F\overline{C}D}$	θ_T	6.076×10^{-2}	$\frac{2\overline{C} h_r}{\tilde{\rho c} T_*}$
θ_β	9.646×10^{-4}	$\frac{2\overline{C}}{C_l R_c}$			

5.6 Reducing the Differential Equations

5.6.1 The Total Gas Expansion

We can expand the total gas concentration expression as follows:

$$\begin{aligned} [CT]_y &= O\left(\frac{1}{R_g}\right) \\ CT &= C(0)T(0) + \frac{P^{(1)}}{R_g} + O\left(\frac{1}{R_g^2}\right) \\ CT &= 1 + \frac{P^{(1)}}{R_g} + O\left(\frac{1}{R_g^2}\right) \end{aligned}$$

In this notation,

$$P_g = R_g CT = R_g + P^{(1)} + O\left(\frac{1}{R_g}\right)$$

and

$$U_g = -\frac{Kk_{rg}(\beta)}{\mu_g} \bigtriangledown P_g = -\frac{Kk_{rg}(\beta)}{\mu_g} \bigtriangledown (P^{(1)}) + O\left(\frac{1}{R_g}\right)$$

Recall, $C(0) = 1$ and $T(0) = 1$ from the boundary conditions. Consequently, we get the following expansion for $C(y)$:

$$\boxed{C(y) = \frac{1}{T(y)} + \frac{P^{(1)}}{R_g T(y)} + O\left(\frac{1}{R_g^2}\right)} \tag{5.11}$$

5.6.2 The Water Vapour Expansion

To determine the correct expansion for the water vapour, let us first examine the definition (3.4) of Γ:

$$\Gamma = H(C_2 - C_2^{sat})$$

Assumption (A4) requires that H is very large. As a result, in order for Γ to still be $O(1)$ (see (A3)) the following must be true:

$$C_2 - C_2^{sat} = O\left(\frac{1}{H}\right) \tag{5.12}$$

Note that the assumption (A3) that $\Gamma = O(1)$ is not inconsistent with the water vapour equation:

$$\left(R_g C_2 [CT]_y + C \left[\frac{C_2}{C} \right]_y \right)_y = \Gamma$$

Since $R_g C_2 [CT]_y = C_2 P^{(1)} \leq O(1)$ and $C \left[\frac{C_2}{C} \right]_y \leq O(1)$.
The expression (5.12) leads to the following expansion:

$$\boxed{C_2 = C_2^{sat}(T) + \frac{1}{H} C_2^{(1)} + O\left(\frac{1}{H^2}\right)} \tag{5.13}$$

The assumptions (A3) and (A4) also imply that the water vapour is very near saturation. As well, the expansion (5.13) for C_2 provides the following expansion for Γ:

$$\begin{aligned} \Gamma &= H(C_2 - C_2^{sat}) = H\left(C_2^{sat} + \frac{1}{H} C_2^{(1)} + O\left(\frac{1}{H^2}\right) - C_2^{sat} \right) \\ &= C_2^{(1)} + O\left(\frac{1}{H}\right) \end{aligned} \tag{5.14}$$

Now, we employ the assumptions and the expansions to reduce our system of equations and boundary conditions.

5.7 Reducing the differential equations

5.7.1 The reduced oxygen equation

Let us start with the oxygen equation (5.1) at steady-state:

$$-\left(R_g C_1 [CT]_y + C \left[\frac{C_1}{C} \right]_y \right)_y = 0$$

Now, let us add in the total gas concentration and water vapour expansions and group $O\left(\frac{1}{R_g^2}\right)$ terms with the $O\left(\frac{1}{R_g}\right)$ terms:

$$\begin{aligned}
0 &= \left(R_g C_1 \left[1 + \frac{P^{(1)}}{R_g} + O\left(\frac{1}{R_g^2}\right) \right]_y + \left[\frac{1}{T} + \frac{1}{R_g}\frac{P^{(1)}}{T} + O\left(\frac{1}{R_g^2}\right) \right] \left[\frac{C_1}{\frac{1}{T} + \frac{1}{R_g}\frac{P^{(1)}}{T} + O\left(\frac{1}{R_g^2}\right)} \right]_y \right)_y \\
&= \left(R_g C_1 \left[0 + \frac{P^{(1)}}{R_g} + O\left(\frac{1}{R_g^2}\right) \right]_y + \left[\frac{1}{T} + O\left(\frac{1}{R_g}\right) \right] \left[\frac{C_1}{\frac{1}{T} + O\left(\frac{1}{R_g}\right)} \right]_y \right)_y \\
&= \left((C_1 P_y^{(1)}) + \left(\frac{1}{T}[TC_1]_y \right)_y + O\left(\frac{1}{R_g}\right) \right)_y
\end{aligned}$$

We integrate both sides and recall the constant of integration is $d_1 = -I_0$ (see (5.7)).

$$\boxed{(C_1 P_y^{(1)}) + \tfrac{1}{T}[TC_1]_y + O\left(\tfrac{1}{R_g}\right) = -I_0} \tag{5.15}$$

5.7.2 The reduced water vapour equation

Let us start with the water vapour equation (5.2) at steady-state:

$$-\left(R_g C_2 [CT]_y + C \left[\frac{C_2}{C} \right]_y \right)_y = -\Gamma$$

Now, if we plug in the expansions for $C(y)$ and $C_2(y)$ - (5.11) and (5.13) respectively, we get the following expression:

$$\begin{aligned}
&-\left(R_g \left(C_2^{sat} + \frac{1}{H} C_2^{(1)} + O\left(\frac{1}{H^2}\right) \right) \left[1 + \frac{1}{R_g} P^{(1)} + O\left(\frac{1}{R_g^2}\right) \right]_y + \right. \\
&\left. + \left(1 - \frac{T^{(1)}}{T_*} + O\left(\frac{I_0}{R_g}, \frac{1}{T_*^2}, \frac{1}{R_g^2}\right) \right) \left[\frac{\left(C_2^{sat} + \frac{1}{H} C_2^{(1)} + O\left(\frac{1}{H^2}\right) \right)}{\left(1 - \frac{T^{(1)}}{T_*} + O\left(\frac{I_0}{R_g}, \frac{1}{T_*^2}, \frac{1}{R_g^2}\right) \right)} \right]_y \right)_y = -\Gamma
\end{aligned}$$

Now, we factor the R_g into the first term and drop the second order terms:

$$\left(\left(C_2^{sat} + O\left(\frac{1}{H}\right) \right) \left[R_g + P^{(1)} + O\left(\frac{1}{R_g}\right) \right]_y + \left(\frac{1}{T} + O\left(\frac{1}{R_g}\right) \right) \left[\frac{\left(C_2^{sat} + O\left(\frac{1}{H}\right) \right)}{\left(\frac{1}{T} + O\left(\frac{1}{R_g}\right) \right)} \right]_y \right)_y = \Gamma$$

Then, we take the derivative in the first term and bring out the $O\left(\frac{1}{R_g}\right)$ and $O\left(\frac{1}{H}\right)$ terms.

$$\boxed{\left(C_2^{sat}P_y^{(1)} + \tfrac{1}{T}[TC_2^{sat}]_y\right)_y + O\left(\tfrac{1}{H}, \tfrac{1}{R_g}\right) = \Gamma} \tag{5.16}$$

From the expansion (5.13), we see that (5.16) is an expression for the water vapour correction $C_2^{(1)}$:

$$\boxed{C_2^{(1)} = \left(C_2^{sat}P_y^{(1)} + \tfrac{1}{T}[TC_2^{sat}]_y\right)_y + O\left(\tfrac{1}{H}, \tfrac{1}{R_g}\right)} \tag{5.17}$$

5.7.3 The Reduced Total Gas Equation

Let us start with steady-state total gas equation

$$-\left(R_g C[CT]_y\right)_y = -\Gamma$$

Plugging in the expansions for $C(y)$ and $C_2(y)$ and the expression for Γ (5.13) gives the following:

$$-\left(R_g\left(1 - \frac{T^{(1)}}{T_*} + O\left(\frac{I_0}{R_g}, \frac{1}{T_*^2}, \frac{1}{R_g^2}\right)\right)\left[1 + \frac{1}{R_g}P^{(1)} + O\left(\frac{1}{R_g^2}\right)\right]_y\right)_y = -C_2^{(1)} + O\left(\frac{1}{H}\right)$$

Now, factoring the R_g term into $[CT]_y$ and dropping the second order terms gives:

$$\left(\left(\frac{1}{T} + O\left(\frac{1}{R_g}\right)\right)\left[R_g + P^{(1)} + O\left(\frac{1}{R_g}\right)\right]_y\right)_y = C_2^{(1)} + O\left(\frac{1}{H}\right)$$

Finally, taking the derivative of the second term and bringing out the $O\left(\frac{1}{R_g}\right)$ terms gives:

$$\boxed{\left(\tfrac{P_y^{(1)}}{T}\right)_y = C_2^{(1)} + O\left(\tfrac{1}{H}, \tfrac{1}{R_g}\right)} \tag{5.18}$$

5.7.4 The Reduced Liquid Water Equation

Let us start with the water equation at steady-state

$$-\left(R_l\beta k_{rl}(\beta)[CT]_y + R_c f(\beta)\beta_y\right)_y = \delta_l\Gamma$$

Plugging in the expansions for $C(y)$ and Γ - (5.11) and (5.13) respectively - gives:

$$-\left(R_l\beta k_{rl}(\beta)\left[1+\frac{1}{R_g}P^{(1)}+O\left(\frac{1}{R_g^2}\right)\right]_y+R_cf(\beta)\beta_y\right)_y=\delta_l\left(C_2^{(1)}+O\left(\frac{1}{H}\right)\right)$$

Taking the derivative in the first term and bringing out the $O\left(\frac{1}{R_g^2}\right)$ and $O\left(\frac{\delta_l}{H}\right)$ terms gives:

$$\left(R_l\beta k_{rl}(\beta)\frac{P_y^{(1)}}{R_g}+R_cf(\beta)\beta_y\right)_y+O\left(\frac{1}{R_g^2}\right)=-\delta_lC_2^{(1)}+$$

Since $\delta_l = O(10^{-3})$, we will group $\delta_l\Gamma$ with the $O\left(\frac{1}{R_g}\right)$ term (the first term in the equation). We will also now neglect the $O\left(\frac{1}{R_g^2}\right)$ and $\delta_lO\left(\frac{1}{H}\right)$ terms, which gives:

$$\boxed{(R_cf(\beta)\beta_y)_y=O\left(\delta_l,\frac{1}{R_g}\right)} \tag{5.19}$$

5.7.5 The Reduced Temperature Equation

Let us start with the steady-state temperature equation

$$-\left(r_gT[CT]_y+r_l\beta k_{rl}(\beta)T[CT]_y+r_cf(\beta)\beta_yT+F_bT_y\right)_y=\delta_T\Gamma$$

Plugging in the expansions (5.11) and (5.13) gives:

$$-\left(r_gT\left[1+\frac{1}{R_g}P^{(1)}+O\left(\frac{1}{R_g^2}\right)\right]_y+r_l\beta k_{rl}(\beta)T\left[1+\frac{1}{R_g}P^{(1)}+O\left(\frac{1}{R_g^2}\right)\right]_y\right.$$
$$\left.+\ r_cf(\beta)\beta_yT+F_bT_y\right)_y=\delta_T\left(C_2^{(1)}+O\left(\frac{1}{H}\right)\right)$$

We now take the derivative of the first and second terms and neglect the $O\left(\frac{1}{R_g^2}\right)$ and $\delta_TO\left(\frac{1}{H}\right)$ terms:

$$\left(\frac{r_g}{R_g}TP_y^{(1)}+\frac{r_l}{R_g}\beta k_{rl}(\beta)TP_y^{(1)}+r_cf(\beta)\beta_yT+F_bT_y\right)_y=-\delta_TC_2^{(1)}$$

Keeping only the highest order terms:

$$\boxed{(r_cf(\beta)\beta_yT+F_bT_y)_y=O\left(\delta_T,\frac{1}{R_g}\right)} \tag{5.20}$$

5.8 Reducing the Boundary Conditions

5.8.1 The Oxygen Boundary Condition at the Catalyst Layer

We start with oxygen boundary condition at the channel as expressed (4.5):

$$\left[R_g k_{rg}(\beta) C_1 [CT]_y + C\left[\frac{C_1}{C}\right]_y\right]_{y=1} = -I_0$$

Now, plugging in the asymptotic expansion for $C(y)$ gives:

$$\left[k_{rg}(\beta) C_1 \left[P_y^{(1)} + O\left(\frac{1}{R_g}\right)\right] + \left(\frac{1}{T} + O\left(\frac{1}{R_g}\right)\right)\left[\frac{C_1}{\left(\frac{1}{T} + O\left(\frac{1}{R_g}\right)\right)}\right]_y\right]_{y=1} = -I_0$$

Grouping the $O\left(\frac{1}{R_g}\right)$ terms and plugging in the previous approximation, $k_{rg}(\beta) \approx 1$,the above equation becomes:

$$\boxed{C_1 P_y^{(1)} + \tfrac{1}{T}[TC_1]_y + O\left(\tfrac{1}{R_g}\right) = -I_0} \tag{5.21}$$

The oxygen boundary condition at the channel does not need to be reduced.

5.8.2 The Water Vapour Boundary Condition at the Catalyst Layer

At the catalyst layer, we will start with the boundary condition (4.10):

$$\left[R_g k_{rg}(\beta) C_2 [CT]_y + C\left[\frac{C_2}{C}\right]_y\right]_{y=1} = 2(1+\nu) I_0$$

Plugging in the expansions for $C_2(y)$ and $C(y)$, the boundary condition becomes:

$$\left[k_{rg}(\beta)\left(C_2^{sat} + O\left(\frac{1}{H}\right)\right)\left[P_y^{(1)} + O\left(\frac{1}{R_g}\right)\right] + \left[\frac{\left(C_2^{sat} + O\left(\frac{1}{H}\right)\right)}{\left(\frac{1}{T} + O\left(\frac{1}{R_g}\right)\right)}\right]_y\right]_{y=1} = 2(1+\nu) I_0$$

Grouping the $O\left(\frac{1}{R_g}\right)$ and $O\left(\frac{1}{H}\right)$ terms and plugging in the approximation $k_{rl}(\beta) \approx 1$ gives:

$$\boxed{\left[C_2^{sat} P_y^{(1)} + \tfrac{1}{T}[TC_2^{sat}]_y + O\left(\tfrac{1}{H}, \tfrac{1}{R_g}\right)\right]_{y=1} = 2(1+\nu) I_0} \tag{5.22}$$

5.8.3 The Total Gas Boundary Condition at the Catalyst Layer

Let us start with the boundary condition at the catalyst layer (4.15):

$$[R_g k_{rg}(\beta) C[CT]_y]_{y=1} = (1+2\nu)I_0$$

Plugging in the expansion for $C(y)$ gives:

$$\left[k_{rg}(\beta)\left(\frac{1}{T}+O\left(\frac{1}{R_g}\right)\right)\left[P_y^{(1)}+O\left(\frac{1}{R_g}\right)\right]\right]_{y=1} = (1+2\nu)I_0$$

Bringing out the $O\left(\frac{1}{R_g}\right)$ terms and plugging in the assumption $k_{rl}(\beta) \approx 1$ gives:

$$\boxed{\left[\frac{1}{T}P_y^{(1)}\right]_{y=1} = (1+2\nu)I_0 + O\left(\frac{1}{R_g}\right)} \tag{5.23}$$

5.8.4 The Liquid Water Boundary Condition at the Channel

Let us start with the liquid water boundary condition at the channel (4.18):

$$\left[\frac{R_l}{R_c}\beta k_{rl}(\beta)[CT]_y + f(\beta)\beta_y\right]_{y=0} = \left[\frac{L}{L_p}k_{rl}(\beta)\mathcal{J}(\beta)\right]_{y=0}$$

Plugging in the expansion for $C(y)$ gives:

$$\left[\frac{R_l}{R_c}\beta k_{rl}(\beta)\left[\frac{P_y^{(1)}}{R_g}+O\left(\frac{1}{R_g^2}\right)\right]+f(\beta)\beta_y\right]_{y=0} = \left[\frac{L}{L_p}k_{rl}(\beta)\mathcal{J}(\beta)\right]_{y=0}$$

Keeping only the highest order terms gives the following boundary condition:

$$\boxed{[f(\beta)\beta_y]_{y=0} + O\left(\frac{1}{R_g}\right) = \left[\frac{L}{L_p}k_{rl}(\beta)\mathcal{J}(\beta)\right]_{y=0}} \tag{5.24}$$

5.8.5 The Liquid Water Boundary Condition at the Catalyst Layer

We start with the boundary condition (4.22)

$$\left[\frac{R_l}{R_c}\beta k_{rl}(\beta)[CT]_y + f(\beta)\beta_y\right]_{y=1} = -\nu\theta_\beta I_0$$

We then plug in the $C(y)$ expansion,

$$\left[\frac{R_l}{R_c}\beta k_{rl}(\beta)\left[\frac{P_y^{(1)}}{R_g}+O\left(\frac{1}{R_g^2}\right)\right]+f(\beta)\beta_y\right]_{y=1}=-\nu\theta_\beta I_0$$

Now, plugging in the approximation $k_{rl}(\beta)\approx 1$ and keeping only the highest order terms gives:

$$\boxed{[f(\beta)\beta_y]_{y=1}=-\nu\theta_\beta I_0+O\left(\tfrac{1}{R_g}\right)} \tag{5.25}$$

5.8.6 The Temperature Boundary Condition at the Catalyst Layer

The boundary condition (4.27) gives:

$$[r_g T[CT]_y+r_l\beta k_{rl}(\beta)T[CT]_y+r_c f(\beta)\beta_y T+F_b T_y]_{y=1}=\left(1-\frac{h_v}{h_r}\nu\right)\theta_T I_0$$

Plugging in the expansion for $C(y)$ gives:

$$\left[r_g T\left(\frac{P_y^{(1)}}{R_g}+O\left(\frac{1}{R_g^2}\right)\right)+r_l\beta k_{rl}(\beta)T\left(\frac{P_y^{(1)}}{R_g}+O\left(\frac{1}{R_g^2}\right)\right)+r_c f(\beta)\beta_y T+F_b T_y\right]_{y=1}=\left(1-\frac{h_v}{h_r}\nu\right)\theta_T I_0$$

Keeping only the highest order terms and plugging in the approximation $k_{rl}(\beta)\approx 1$ gives:

$$\boxed{[r_c f(\beta)\beta_y T+F_b T_y]_{y=1}+O\left(\tfrac{1}{R_g}\right)=(1-\tfrac{h_v}{h_r}\nu)\theta_T I_0} \tag{5.26}$$

5.9 The Resulting Differential Equations at Steady State

Here is the summary of the equations and their boundary conditions that we have derived so far. Please note that there are five unknowns for the five equations at leading order: C_1, $C_2^{(1)}$, $P^{(1)}$, β and T

$$\begin{cases} (C_1 P_y^{(1)}) + \frac{1}{T}[TC_1]_y + O\left(\frac{1}{R_g}\right) = d_1 \\ C_1(0) = 0.2 \\ \left[C_1 P_y^{(1)} + \frac{1}{T}[TC_1]_y\right]_{y=1} + O\left(\frac{1}{R_g}\right) = -I_0 \end{cases} \tag{5.27}$$

$$\begin{cases} \left(C_2^{sat} P_y^{(1)} + \frac{1}{T}[TC_2^{sat}]_y\right)_y + O\left(\frac{1}{H}, \frac{1}{R_g}\right) = C_2^{(1)} \\ C_2(0) = C_2^{sat}(T(0)) \\ \left[C_2^{sat} P_y^{(1)} + \frac{1}{T}[TC_2^{sat}]_y + O\left(\frac{1}{H}, \frac{1}{R_g}\right)\right]_{y=1} = 2(1+\nu) I_0 \end{cases} \tag{5.28}$$

$$\begin{cases} \left(\frac{P_y^{(1)}}{T}\right)_y + O\left(\frac{1}{H}, \frac{1}{R_g}\right) = C_2^{(1)} \\ C(0) = 1 \\ \left[\frac{1}{T} P_y^{(1)}\right]_{y=1} = (1+2\nu) I_0 + O\left(\frac{1}{R_g}\right) \end{cases} \tag{5.29}$$

$$\begin{cases} (R_c f(\beta)\beta_y)_y = O\left(\delta_l, \frac{1}{R_g}\right) \\ \left[\frac{1}{L}\mathcal{J}'(\beta)\beta_y\right]_{y=0} + O\left(\frac{1}{R_g}\right) = \left[\frac{1}{L_p}\mathcal{J}(\beta)\right]_{y=0} \\ [f(\beta)\beta_y]_{y=1} = -\nu\theta_\beta I_0 + O\left(\frac{1}{R_g}\right) \end{cases} \tag{5.30}$$

$$\begin{cases} (r_c f(\beta)\beta_y T + F_b T_y)_y = O\left(\delta_T, \frac{1}{R_g}\right) \\ T(0) = 1 \\ [r_c f(\beta)\beta_y T + F_b T_y]_{y=1} + O\left(\frac{1}{R_g}\right) = (1 - \frac{h_u}{h_r}\nu)\theta_T I_0 \end{cases} \tag{5.31}$$

Chapter 6

The Outer Solutions at Steady-State

Note: The lower case constants in the following section are all constants of integration and they are as follows: a_1, b_1, c_1, c_2 and d_1. All but b_1 and d_1 are dependent upon ν, which will be determined close to the end of this section.

6.1 Solving for the Liquid Water Volume Fraction.

Let us start with (5.19):

$$(R_c f(\beta)\beta_y)_y = O\left(\delta_l, \frac{1}{R_g}\right)$$

Integrating this equation once gives:

$$f(\beta)\beta_y = c_1 + O\left(\delta_l, \frac{1}{R_g}\right) \tag{6.1}$$

Now, let $F(\beta) = \int f(\beta)\beta_y dy$ and then integrate both sides of (6.1):

$$F(\beta) = c_1 y + c_2$$

We can now solve for β up to leading order:

$$\boxed{\beta = F^{-1}(c_1 y + c_2)} \tag{6.2}$$

In order to solve for the constants of integration, we will again use the boundary conditions at y=0 and 1. First, we will solve for c_1 with the boundary condition at y=1 - see (5.25)

$$f(\beta)\beta_y|_{y=1} = -\nu\theta_\beta I_0$$

Note: (6.1) gives $f(\beta)\beta_y = c_1$ up to leading order. Plugging this into the boundary condition gives :

$$\boxed{c_1 = -\nu\theta_\beta I_0 + O\left(\frac{1}{R_g}\right)} \tag{6.3}$$

In order to now solve for c_2, we will use the boundary condition at y=0 (5.24):

$$\begin{aligned} \frac{1}{L_p}\mathcal{J}(\beta)|_{y=0} &= \frac{1}{L}\beta\mathcal{J}'(\beta)\beta_y|_{y=0} \qquad (6.4)\\ \frac{1}{L_p}k_{rl}(\beta)\mathcal{J}(\beta)|_{y=0} &= \frac{1}{L}\beta k_{rl}(\beta)\mathcal{J}'(\beta)\beta_y|_{y=0} \\ &= \frac{1}{L}f(\beta)\beta_y \\ &= \frac{1}{L}c_1 \\ &= -\frac{\nu\theta_\beta I_0}{L} \end{aligned}$$

From (6.2) we know that $F(\beta(0)) = c_2$, and we can solve for $\beta(0)$ from (6.4). In order to do so, let us first rename $k_{rl}(\beta)\mathcal{J}(\beta)$:

$$j(\beta) = k_{rl}(\beta)\mathcal{J}(\beta) \tag{6.5}$$

From (6.5) and the boundary condition (6.4), we can now solve for $\beta(0)$:

$$\beta(0) = j^{-1}\left(\frac{L_p}{L}c_1\right) \tag{6.6}$$

And finally, from (6.6) and the fact that $c_2 = F(\beta(0))$, we can solve for c_2:

$$\boxed{c_2 = F\left(j^{-1}\left(-\frac{L_p\nu\theta_\beta I_0}{L}\right)\right)} \tag{6.7}$$

6.2 Solving for T

Starting with (5.31):

$$(r_c f(\beta)\beta_y T + F_b T_y)_y + O\left(\frac{1}{R_g}\right) = -\delta_T \Gamma$$

Since $\delta_T \ll 1$ (A7), we neglect it when solving for $T(y)$ to leading order. Therefore,

$$(r_c f(\beta)\beta_y T + F_b T_y)_y = O\left(\delta_T, \frac{1}{R_g}\right)$$

Next, we expand out the derivative terms:

$$r_c (f(\beta)\beta_y)_y T + f(\beta)\beta_y T + F_b T_{yy} = O\left(\delta_T, \frac{1}{R_g}\right)$$

Plugging in the expansions for $f(\beta)\beta_y$ and $(f(\beta)\beta_y)_y$ from (5.19) and (6.1) we get the following expansion for the temperature equation:

$$\frac{r_c}{R_c} O\left(\delta_l, \frac{1}{R_g}\right) T + r_c \left(c_1 + O\left(\delta_l, \frac{1}{R_g}\right)\right) T_y + F_b T_{yy} = O\left(\delta_T, \frac{1}{R_g}\right)$$

Since $\frac{r_c}{R_c} T = O(1)$ (see the table of constants), the first term is $O\left(\delta_l, \frac{1}{R_g}\right)$ and we will group it with the other small terms:

$$r_c c_1 T_y + F_b T_{yy} = O\left(\delta_l, \delta_T, \frac{1}{R_g}\right)$$

Integrating the above equation once gives:

$$F_b T_y + r_c c_1 T = O\left(\delta_l, \delta_T, \frac{1}{R_g}\right) + a_1 \tag{6.8}$$

The boundary condition at the catalyst layer (5.26) with $f(\beta)\beta_y$ replaced by c_1 gives:

$$[r_c c_1 T + F_b T_y]_{y=1} = (1 - \frac{h_v}{h_r}\nu)\theta_T I_0$$

With the above equation and (6.8), we may solve for $a_1 = a_1(\nu)$.

$$\boxed{a_1(\nu) = (1 - \tfrac{h_v}{h_r}\nu)\theta_T I_0} \tag{6.9}$$

Using separation of variables, we can solve for $T(y)$:

$$\begin{aligned}
T_y &= \frac{O\left(\delta_l, \delta_T, \frac{1}{R_g}\right) + a_1 - r_c c_1 T}{F_b} \\
\int_{T(0)}^{T(y)} \frac{dT}{O\left(\delta_l, \delta_T, \frac{1}{R_g}\right) + a_1 - r_c c_1 T} &= \int_0^y \frac{1}{F_b} d\overline{y} \\
-\frac{ln\left(\frac{O\left(\delta_l, \delta_T, \frac{1}{R_g}\right) + a_1 - r_c c_1 T(y)}{O\left(\delta_l, \delta_T, \frac{1}{R_g}\right) + a_1 - r_c c_1 T(0)}\right)}{r_c c_1} &= \frac{y}{F_b} \\
\frac{O\left(\delta_l, \delta_T, \frac{1}{R_g}\right) + a_1 - r_c c_1 T(y)}{O\left(\delta_l, \delta_T, \frac{1}{R_g}\right) + a_1 - r_c c_1 T(0)} &= e^{-r_c c_1 y/F_b} \\
O\left(\delta_l, \delta_T, \frac{1}{R_g}\right) + a_1 - r_c c_1 T(y) &= \left(O\left(\delta_l, \delta_T, \frac{1}{R_g}\right) + a_1 - r_c c_1 T(0)\right) e^{-r_c c_1 y/F_b} \\
a_1 - r_c c_1 T(y) &= (a_1 - r_c c_1 T(0)) e^{-r_c c_1 y/F_b} + O\left(\delta_l, \delta_T, \frac{1}{R_g}\right) \\
T(y) &= \frac{1}{r_c c_1}\left(a_1 - (a_1 - r_c c_1 T(0)) e^{-r_c c_1 y/F_b} + O\left(\delta_l, \delta_T, \frac{1}{R_g}\right)\right)
\end{aligned}$$

We now plug in the boundary condition at the channel $T(0) = 1$ and get the following expression for T:

$$\boxed{T(y) = \frac{1}{r_c c_1}\left(a_1 - (a_1 - r_c c_1) e^{-r_c c_1 y/F_b} + O\left(\delta_l, \delta_T, \frac{1}{R_g}\right)\right)} \tag{6.10}$$

6.3 Solving for $P^{(1)}$

Subtracting (5.29) from (5.28), which cancels out $C_2^{(1)}$, we find

$$\left(C_2^{sat} P_y^{(1)} + \frac{1}{T}[T C_2^{sat}]_y - \frac{P_y^{(1)}}{T}\right)_y = O\left(\frac{1}{H}, \frac{1}{R_g}\right) \tag{6.11}$$

Integrating both sides gives:

$$C_2^{sat} P_y^{(1)} + \frac{1}{T}[T C_2^{sat}]_y = \frac{P_y^{(1)}}{T} + b_1 + O\left(\frac{1}{H}, \frac{1}{R_g}\right) \tag{6.12}$$

We can solve for b_1 with the boundary conditions for the water vapour and total gas fluxes at the catalyst layer (y=1) - (5.22) and (5.23).

$$\begin{aligned}\left[C_2^{sat}P_y^{(1)} + \frac{1}{T}[TC_2^{sat}]_y\right]_{y=1} + O\left(\frac{1}{H}, \frac{1}{R_g}\right) &= 2(1+\nu)I_0 \\ \left[\frac{P_y^{(1)}}{T}\right]_{y=1} + O\left(\frac{1}{R_g}\right) &= (1+2\nu)I_0\end{aligned}$$

Plugging both these boundary conditions into (6.12) gives:

$$b_1 = 2(1+\nu)I_0 - (1+2\nu)I_0$$

Which can be simplified down to

$$\boxed{b_1 = I_0} \tag{6.13}$$

Note: b_1 is independent of ν and it is also equal to the oxygen concentration flux.

Now that we have solved for b_1, we can continue to solve for $P^{(1)}(y)$. In order to do this, we can rewrite (6.12) as an expression $P_y^{(1)}$:

$$P_y^{(1)} = \frac{I_0 - \frac{1}{T}[TC_2^{sat}]_y + O\left(\frac{1}{H}, \frac{1}{R_g}\right)}{C_2^{sat} - \frac{1}{T}}$$

Integrating this expression with respect to y gives:

$$P^{(1)}(y) - P^{(1)}(0) = \int_0^y \frac{I_0 - \frac{1}{T}[TC_2^{sat}]_y}{C_2^{sat} - \frac{1}{T}} d\overline{y} + O\left(\frac{1}{H}, \frac{1}{R_g}\right)$$

Multiplying both the top and bottom of the fraction within the integral by T and applying the boundary condition $P^{(1)}(0) = 0$, we get the following expression for $P^{(1)}(y)$:

$$P^{(1)}(y) = \int_0^y \frac{I_0 T - [TC_2^{sat}]_y}{TC_2^{sat} - 1} d\overline{y} + O\left(\frac{1}{H}, \frac{1}{R_g}\right)$$

which can be reduced to:

$$P^{(1)}(y) = \int_0^y \frac{I_0 T}{TC_2^{sat} - 1} d\overline{y} - \int_0^y \frac{[TC_2^{sat}]_y}{TC_2^{sat} - 1} d\overline{y}$$

Which gives:

$$\boxed{P^{(1)}(y) = \int_0^y \frac{I_0 T}{TC_2^{sat} - 1} d\overline{y} - ln\left(1 - TC_2^{sat}\right)\Big|_0^y} \tag{6.14}$$

It is useful to know where $P_y^{(1)}(1) > 0$. Since $P_y^{(1)}(1)$ depends on both ν and I_0, we will include a contour plot of $P_y^{(1)}(1)(\nu, I_0)$ (Figure 6.1). We can notice from the plot that $P_y^{(1)}(\nu, I_0) = 0$ when ν is roughly -0.5 (which is roughly the value we determine for ν in the next section).

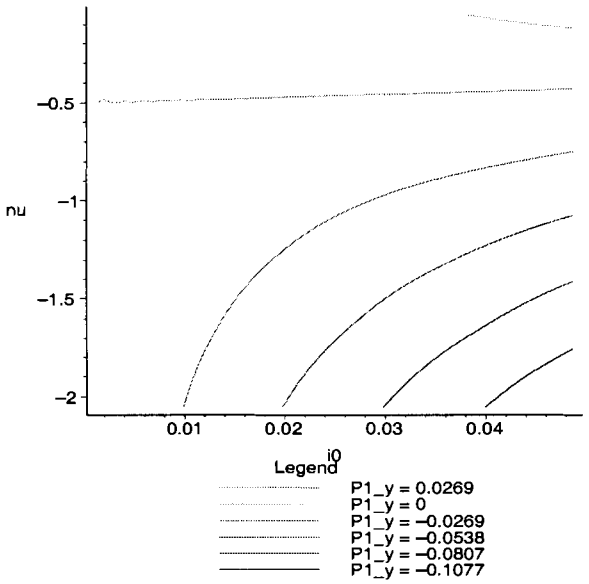

Figure 6.1: Contour plot of $P_y^{(1)}(\nu, I_0)$ at y=1, where $\nu \in [-2, 0)$ and $I_0 \in (0, 0.0474]$. On the second contour from the top, where $\nu \approx -0.5$, $P_y^{(1)} = 0$.

6.4 Solving for ν

As discussed in the introduction, ν is a parameter in our model that is prescribed by the assumption that the water vapour is at saturation and that we have no boundary layer at the catalyst layer. Therefore, ν can be solved by the water vapour boundary condition at the catalyst layer (5.22):

$$C_2^{sat}(T(1))P_y^{(1)}(1) + \frac{1}{T(1)}[TC_2^{sat}]_y|_{y=1} = 2(1+\nu)I_0 + O\left(\frac{1}{H}, \frac{1}{R_g}\right) \tag{6.15}$$

Please note that both $T(y)$ and $P_y^{(1)}(y)$ depend upon ν since both of their boundary conditions at y=1 depend upon ν. Let us rewrite both $T(1)$ and $P_y^{(1)}(1)$ as functions of ν:

$$\begin{aligned} T(1,\nu) &= \frac{1}{r_c c_1(\nu)}\left[a_1(\nu) - (a_1(\nu) - r_c c_1(\nu))e^{-\frac{r_c c_1(\nu)}{F_b}} + O\left(\delta_l, \delta_T, \frac{1}{R_g}\right)\right] \\ P_y^{(1)}(1,\nu) &= \frac{I_0 - \frac{1}{T(1,\nu)}[T(1,\nu)C_2^{sat}(T(1,\nu))]_y}{C_2^{sat}(T(1,\nu)) - \frac{1}{T(1,\nu)}} \end{aligned}$$

where $a_1(\nu)$ and $c_1(\nu)$ are also functions of ν given by (6.9) and (6.1) respectively,

$$\begin{aligned} a_1(\nu) &= (1 - \frac{h_v}{h_r}\nu)\theta_T I_0 \\ c_1(\nu) &= -\nu\theta_\beta I_0 \end{aligned}$$

Since the equation for ν (6.15) is nonlinear, we use Maple's built-in solver - which gives: $\boxed{\nu = -0.4877}$. For comparison, let us also examine the contour plot of $P_y^{(1)}$ (Fig.6.1) and the total gas concentration boundary condition at the catalyst layer:

$$\left[\frac{1}{T}P_y^{(1)}\right]_{y=1} = (1 + 2\nu)I_0$$

Note: $P_y^{(1)} = 0$ when $\nu \approx -0.5$ and $(1 + 2\nu)I_0 \approx 0$ when $\nu \approx -0.5$. Therefore, the total gas concentration boundary condition is satified when $\nu \approx= -0.5$ - which is consistent with Maple's result. The solution $\nu \approx -1/2$ is important for two reasons: firstly, it implies that roughly half of the water produced at the membrane condenses. Secondly, it implies that the total gas flux at the catalyst layer is roughly zero.

6.5 The resulting constants of integration

Now that we have determined ν, we can also determine $a_1(\nu)$, $c_1(\nu)$ and $c_2(\nu)$. Given below is a table of all the constants of integration used.

The constants of integration		
a_1	$(1-\frac{h_v}{h_r}\nu)\theta_T I_0$	2.232×10^{-3}
b_1	I_0	2.732×10^{-2}
c_1	$-\nu\theta_\beta I_0$	1.095×10^{-5}
c_2	$F\left(j^{-1}\left(\frac{-L\nu\theta_\beta I_0}{L_p}\right)\right)$	2.045×10^{-9}
d_1	$-I_0$	-2.732×10^{-2}

6.6 Solving for U_g

We can now also solve for the gas velocity, U_g. From (10), we know that

$$U_g = -\frac{Kk_{rg}(\beta)}{\mu_g}[\hat{C}R\hat{T}]_{\hat{y}}$$

Plugging in all the non-dimensional variables and multiplying and dividing by D gives:

$$U_g = -\frac{K\overline{C}RT_*}{D\mu_g}\frac{D}{L}k_{rg}(\beta)[CT]_y$$

Finally, substituting in R_g gives:

$$U_g = -\frac{DR_g}{L}k_{rg}(\beta)[CT]_y \tag{6.16}$$

As we have seen in previous sections:

$$\begin{aligned} R_g[CT]_y &= \left[1 + P^{(1)} + O\left(\frac{1}{R_g}\right)\right]_y \\ &= P_y^{(1)} + O\left(\frac{1}{R_g}\right) \end{aligned}$$

Let us plug the above expression for $R_g[CT]_y$ and the approximation $k_{rg}(\beta) \approx 1$ into (6.16) to get an expression for the total gas velocity:

$$U_g = \frac{-D}{L}(P_y^{(1)} + O\left(\frac{1}{R_g}\right)) \tag{6.17}$$

6.7 Solving for C_1

We will start with the reduced oxygen equation (5.15),

$$(C_1 P_y^{(1)}) + \frac{1}{T}[TC_1]_y = -I_0 + O\left(\frac{1}{R_g}\right)$$

Multiplying both sides by T gives:

$$TC_1 P_y^{(1)} + [TC_1]_y = -I_0 T + O\left(\frac{1}{R_g}\right)$$

Let us now define the following substitution $w = TC_1$ and plug this into the above equation,

$$P_y^{(1)} w + w_y = -I_0 T + O\left(\frac{1}{R_g}\right)$$

Now, multiplying through by the integrating factor $e^{\int_0^y P_{\bar{y}}^{(1)} d\bar{y}}$ gives:

$$\left(e^{\int_0^y P_{\bar{y}}^{(1)} d\bar{y}} w\right)_y = -e^{\int_0^y P_{\bar{y}}^{(1)} d\bar{y}} I_0 T + O\left(\frac{1}{R_g}\right) \tag{6.18}$$

where this integrating factor can be simplified down (please note that $P^{(1)}(0) = 0$):

$$\begin{aligned} e^{\int_0^y P_{\bar{y}}^{(1)} d\bar{y}} &= e^{P^{(1)}(y) - P^{(1)}(0)} \\ &= e^{P^{(1)}(y)} \end{aligned}$$

Plugging in this simplification into (6.18) and integrating gives:

$$e^{P^{(1)}(y)} w - w(0) = -I_0 \int_0^y e^{P^{(1)}(y)} T(\tilde{y}) d\tilde{y} + O\left(\frac{1}{R_g}\right)$$

Now, we can plug back in the expression for w, (TC_1):

$$e^{P^{(1)}(y)} T(y) C_1(y) - T(0) C_1(0) = -I_0 \int_0^y e^{P^{(1)}(y)} T(\tilde{y}) d\tilde{y} + O\left(\frac{1}{R_g}\right)$$

From the boundary conditions at the channel - (4.23) and (4.1), we know that $T(0) = 1$ and $C_1(0) = 0.2$. Plugging these conditions in and solving for $C_1(y)$ gives:

$$\boxed{C_1(y) = \frac{e^{-P^{(1)}(y)}}{T(y)} \left(-I_0 \int_0^y e^{P^{(1)}(y)} T(\tilde{y}) d\tilde{y} + 0.2 + O\left(\frac{1}{R_g}\right)\right)} \tag{6.19}$$

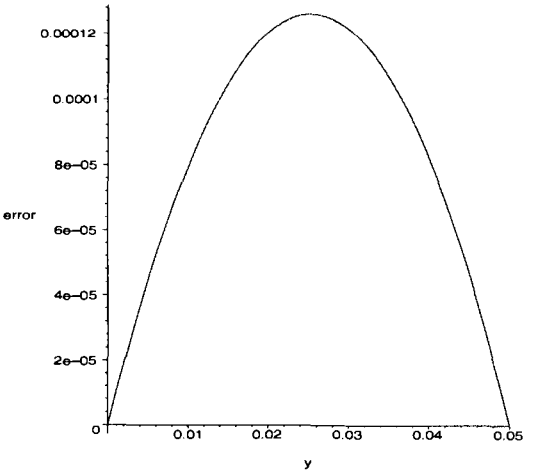

Figure 6.2: Relative error between $T(y)e^{P^{(1)}(y)}$ and its linear approximation across the GDL.

where $I_0 \approx 2.372 \times 10^{-2}$.

Both $T(y)$ and $T(y)e^{P^{(1)}(y)}$ are approximated by linear functions when plotting $C_1(y)$. Fig.6.2 illustrates the error between $T(y)e^{P^{(1)}(y)}$ and its linear approximation. This relative error is $O(10^{-4})$. Consequently, the linear approximation to $T(y)e^{P^{(1)}(y)}$ is not too bad of an approximation.

6.8 Solving for $C_2^{(1)}$

There are two different ways to solve for $C_2^{(1)}$ from the two equations (5.29) and (5.28). We will use both equations and then determine the error (or difference) between them. This error will be due to the fact that we are using a linear approximation for $T(y)$ and the approximation $k_{rg}(\beta) \approx 1$. Let us first solve for $C_2^{(1)}$ from (5.29):

$$C_2^{(1)} = \left(\frac{P_y^{(1)}}{T}\right)_y + O\left(\frac{1}{H}, \frac{1}{R_g}\right)$$

Now, we substitute in the expression for $P^{(1)}$:

$$C_2^{(1)} = \left(\frac{1}{T}\frac{d}{dy}\int_0^y \frac{I_0 T - (TC_2^{sat})_{\overline{y}}}{TC_2^{sat} - 1} d\overline{y}\right)_y + O\left(\frac{1}{H}, \frac{1}{R_g}\right)$$

The fundamental theorem of calculus gives:

$$C_2^{(1)} = \left(\frac{1}{T} \frac{I_0 T - (TC_2^{sat})_{\overline{y}}}{TC_2^{sat} - 1} \right)_y + O\left(\frac{1}{H}, \frac{1}{R_g} \right)$$

Consequently, $C_2^{(1)}$ can be expressed as below and is illustrated in Fig.6.3

$$\boxed{C_2^{(1)} = \left(\frac{I_0 T - (TC_2^{sat})_{\overline{y}}}{T^2 C_2^{sat} - T} \right)_y + O\left(\frac{1}{H}, \frac{1}{R_g} \right)} \tag{6.20}$$

We can now solve for $C_2^{(1)}$ using (5.28):

$$\boxed{C_2^{(1)} = \left(C_2^{sat} P_y^{(1)} + \frac{1}{T}[TC_2^{sat}]_y \right)_y + O\left(\frac{1}{H}, \frac{1}{R_g} \right)} \tag{6.21}$$

Note: We will not write out the explicit solution given from this equation, but we will plot the resulting $C_2^{(1)}$ in the right-hand plot of Fig.6.3. We will also examine the error between the two solutions - as seen in left-hand plot of Fig.6.3.

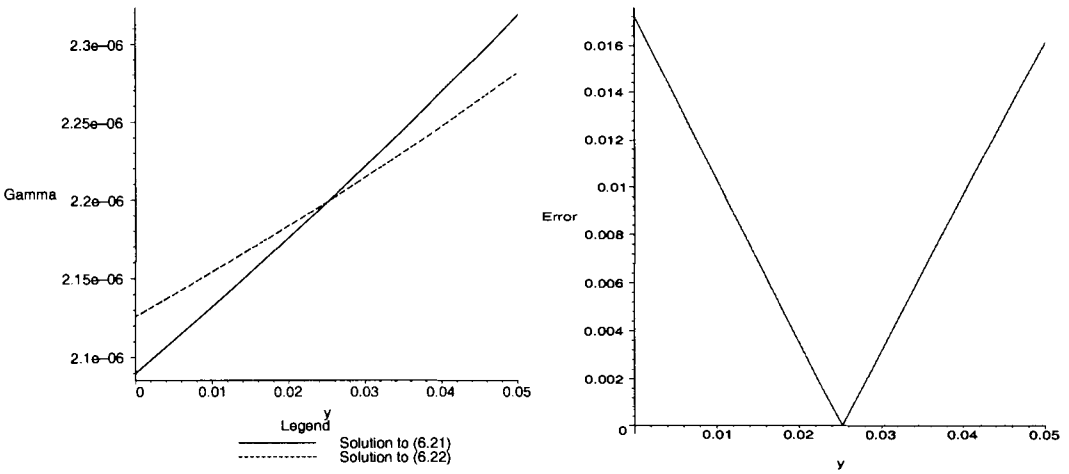

Figure 6.3: The two solutions of $C_2^{(1)}$ - the first correction for the dimensionless water vapour concentration at steady-state - derived from (6.20) and (6.21) and plotted across the GDL (left). The error between the two solutions (right).

From comparing the plots left and right-hand plots Fig.6.3, we can see that the difference between the two solutions is $O(10^{-2})$. Therefore, the relative error is about 1%. Hence, both results are close in value, which strongly implies that our calculations of $T(y)$ and $P^{(1)}$ are correct.

6.9 The Validity of the Assumptions

Now that we have the solutions for the five variables C_1, C_2, C, β and T, let us now examine the assumptions, (A1) through (A3), and check to see whether they are valid assumptions. Please note that (A4) cannot be verified, since we have no way of calculating H explicitly.

The first assumption, (A1), that $\left[ln\frac{C_1}{C}\right]_y = O(1)$ is true. See the left-hand plot in Fig.6.4. The second assumption, (A2), that $C(y) = O(1)$ is also true - in fact, the non-dimensional total gas concentration is almost exactly 1. See the right-hand plot in Fig.6.4.

From the previous section, we know that $C_2^{(1)} = O(10^{-6})$. We also know, from (3.4) that $C_2^{(1)} = \Gamma$ up to leading order. Therefore, assumption (A3) that $\Gamma = O(1)$ or less is also true. Finally, we can also verify (A1) that $\frac{I_0}{C_1} \leq O(1)$ since, from Fig.6.5, we determine that $\frac{I_0}{C_1} \in [0.119, 0.136]$ and therefore, $\frac{I_0}{C_1} \leq O(1)$. Consequently, the assumptions (A1) through (A3) are valid and the solutions we obtain to leading order should also be valid as a result.

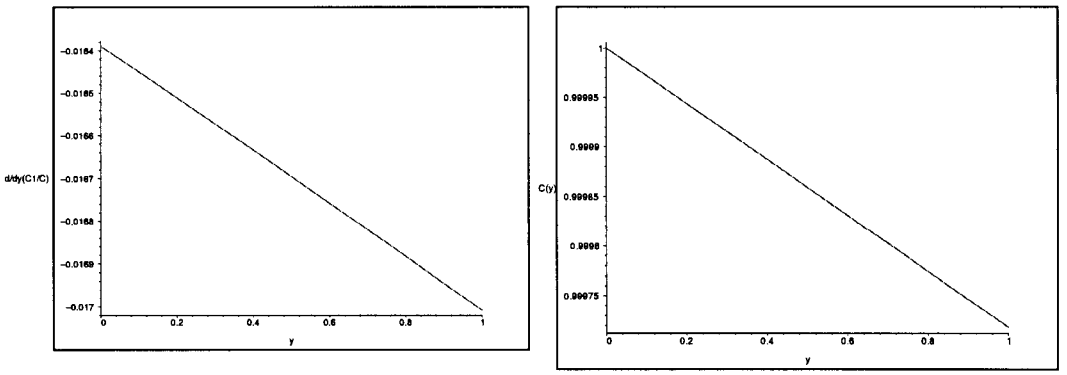

Figure 6.4: $\left[ln\frac{C_1}{C}\right]_y$ (left-hand figure) and $C(y)$ (right-hand figure).

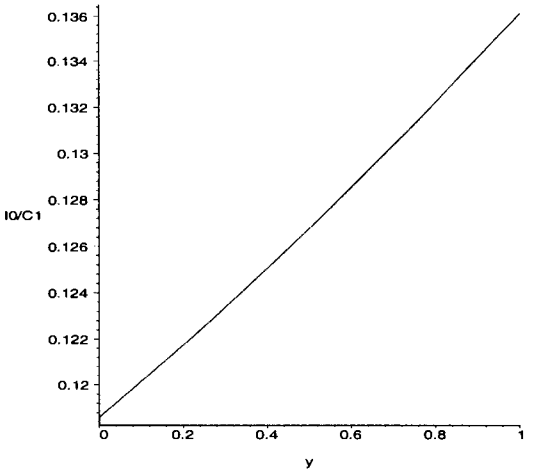

Figure 6.5: $\frac{I_0}{C_1}$ across the GDL.

Chapter 7

Summary of Main Results

There are several interesting studies to perform on our steady-state solutions with the assumption that the entire GDL is at saturation. The first of these studies involves varying the input parameters I, κ_s and T_0 and examining the effects on ν (the percentage of product water manufactured in liquid form).

7.1 Studying ν

The first parameter to vary is I, the current - which we will vary from 0.1 to 2 Amp/cm^2. As we see in Fig.7.1, ν increases with the current and, more importantly, there is a rapid change in ν for $I \in (0, 0.3) Amp/cm^2$. We also observe from Fig. 7.1 that when the current is very low then $\nu < -1$, which implies that more water than produced is condensed in this regime. We finally notice that when we take the current at $I = 1\ Amp/cm^2$, we get the expected value $\nu = -0.4877$ (which implies that roughly half of the water produced condenses). We will discuss several interesting consequences of $\nu \approx -1/2$ in later sections.

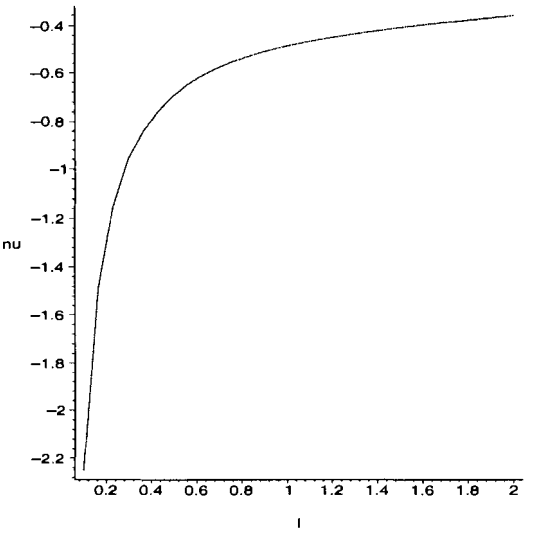

Figure 7.1: The variation in ν with the current, I, at the catalyst layer. The thermal conductivity constant is fixed at $\kappa_s = 10^5 erg/cm \cdot s \cdot K$.

The second parameter to vary is κ_s, the thermal conductivity. As we see in Fig.7.2, ν decreases as κ_s increases. As well, ν changes rapidly while $\kappa_s \in (10^4, 10^5)\ erg/cm\ s\ K$. We also notice that $\nu < -1$ when $\kappa_s > 5 \times 10^5\ erg/cm\ s\ K$.

The third and final parameter to vary is T_0, the channel temperature. We vary this temperature from 323 to 363 K and observe from Fig.7.3 that ν increases with the channel temperature. This result is physical - as the channel becomes hotter, less water will condense and ν will become less negative. An interesting observation to be noted is that ν is not as sensitive to small changes in T_0 as it is to I and κ_s.

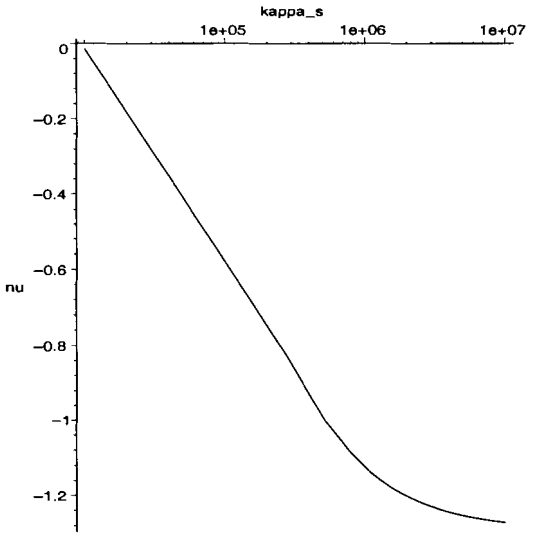

Figure 7.2: The variation in ν with the thermal conductivity, κ_s vs. ν, where the current is fixed at $I = 1Amp/cm^2$.

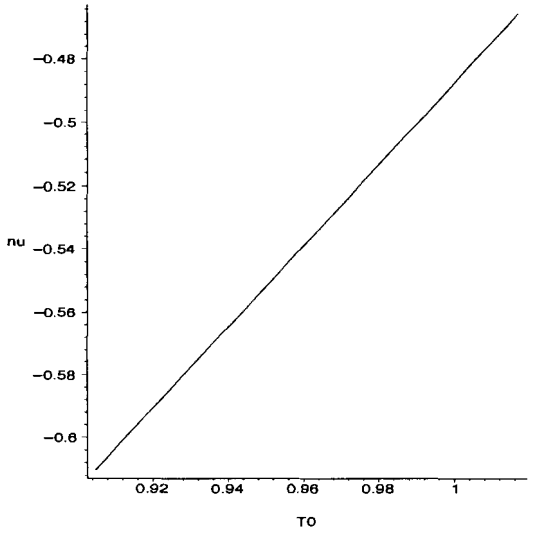

Figure 7.3: The variation in ν with the nondimensional channel temperature, where the current is fixed at $I = 1Amp/cm^2$ and $\kappa_s = 10^5 erg/cm \cdot s \cdot K$.

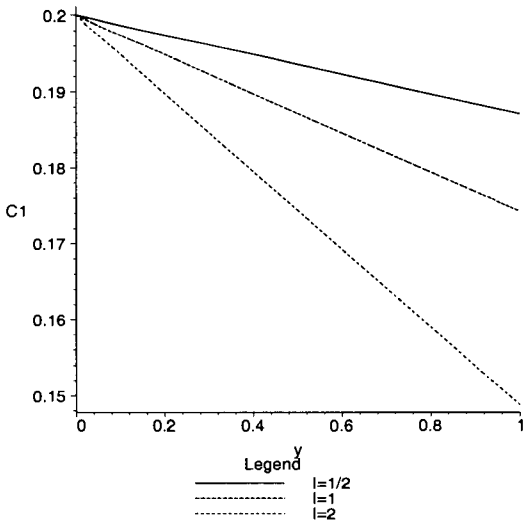

Figure 7.4: The oxygen concentration for 3 different current values: I= 1/2, 1, 2 Amp/cm^2.

7.2 The effects of varying I

Let us now examine the effects of varying I on the oxygen, water vapour, total gas concentration and the temperature. Firstly, we examine the O_2 concentration for different currents. As we see in Figure 7.4, the O_2 concentration decreases as the current increases at the catalyst layer. This result is physical, since a larger current implies that more reactions are taking place at the catalyst layer. Hence, the O_2 concentration will lower as the current increases.

Secondly, we examine the water vapour concentration for 3 different current values. As we see in Figure 7.5, the water vapour concentration increases with the current. This result is reasonable since a larger current implies that more reactions are taking place at the catalyst layer and therefore, more water vapour is being produced in vapour form. The increase in the water vapour concentration with the current can also be explained by examining Fig. 7.1 - which shows that ν becomes less negative as the current increases and therefore more water is produced in vapour form.

Thirdly, we examine the change in the total gas concentration as I varies - shown

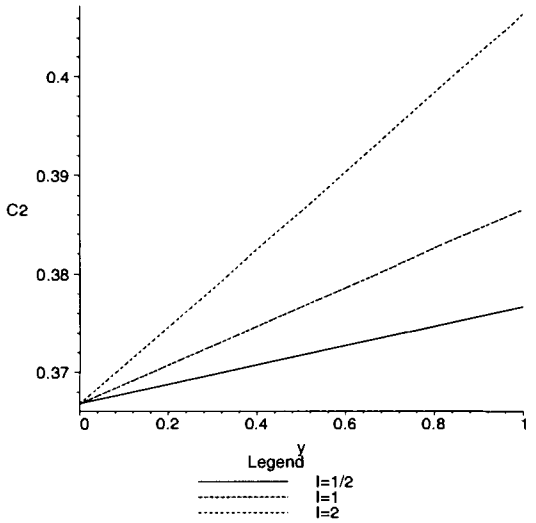

Figure 7.5: The water vapour concentration for 3 different current values: I= 1/2, 1, 2 Amp/cm^2.

in Fig.7.6. We observe from this figure that the total gas concentration decreases as the current increases.

Finally, we examine the temperature distribution as I varies. We observe, in Fig.7.7, that the temperature increases with the current. This effect is due to the heat produced by the reaction - the larger the current, the more reactions occur at the catalyst layer and the higher the temperature there.

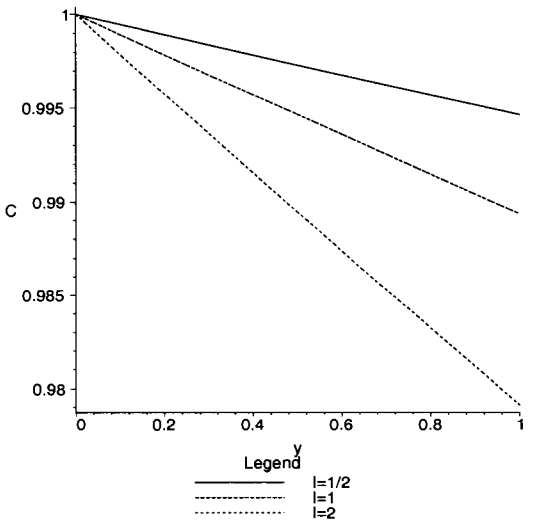

Figure 7.6: The total gas concentration for 3 different current values: I= 1/2, 1, 2 Amp/cm^2.

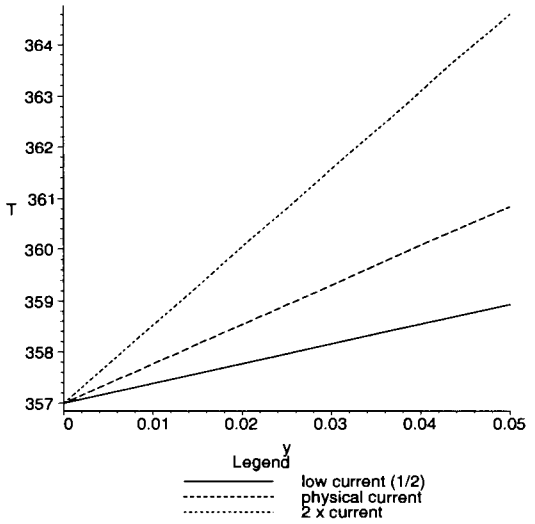

Figure 7.7: The temperature distribution for 3 different current values: I= 1/2, 1, 2 Amp/cm^2.

7.3 The effects of varying κ_S

We will now vary the thermal conductivity constant κ_s, and observe how the gas and temperature distributions are effected. Figures ?? through ?? illustrate the effects of varying the conductivity by factors of 1/2 and 100.

From Fig.??, we observe that the oxygen and total gas concentrations increase at the catalyst layer with κ_s, while the water vapour concentration and temperature decrease as κ_s increases - as seen in Fig. ?? and ??.

The last effect - that the temperature decreases as κ_s increases - can be physically explained. The more conductive the material, the more heat will be conducted away and the lower the temperature in the GDL will be. The effects on the total gas concentration follow from the temperature distribution. The total gas concentration, $C(y)$ is inversely proportional to the temperature. Therefore, as T decreases with κ_s, C increases.

The decrease in the water vapour concentration as κ_S increases can also be explained by the temperature distribution. The lowest conductivity produces the largest temperature gradient across the channel and therefore causes the most evaporation from the channel to the catalyst layer. For this reason, the water vapour concentration is the highest for the lowest κ_s.

Finally, the increase in O_2 concentration with κ_s is less intuitive to understand (see Fig. ??). Instead, we can note that for the fuel cell - a larger κ_s seems favorable since more O_2 is present with higher κ_s and therefore more O_2 is available for the reactions that produce useful potential energy. As we will later conclude, the oxygen concentration is not the only effect to examine to determine the efficiency of the fuel cell (and therefore, $\kappa_s = 10^7$ might not be optimum).

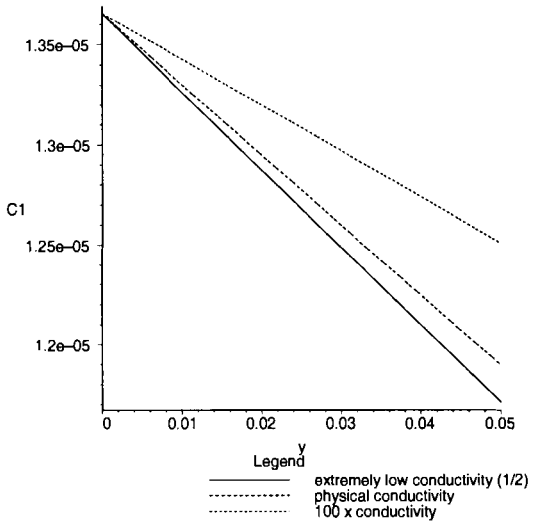

Figure 7.8: The oxygen concentration for 3 different thermal conductivity values: $\kappa_s = 5 \times 10^4$, 10^5, 10^7 $erg/cm \cdot s \cdot K$, where I is fixed at 1 Amp/cm^2.

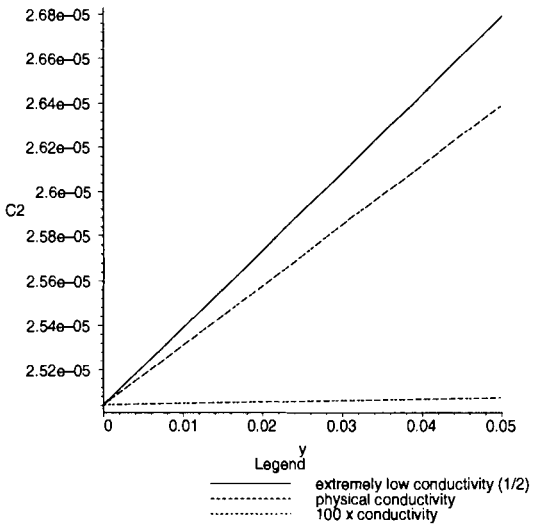

Figure 7.9: The water vapour concentration for 3 different thermal conductivity values: $\kappa_s = 5 \times 10^4$, 10^5, 10^7 $erg/cm \cdot s \cdot K$, where I is fixed at 1 Amp/cm^2.

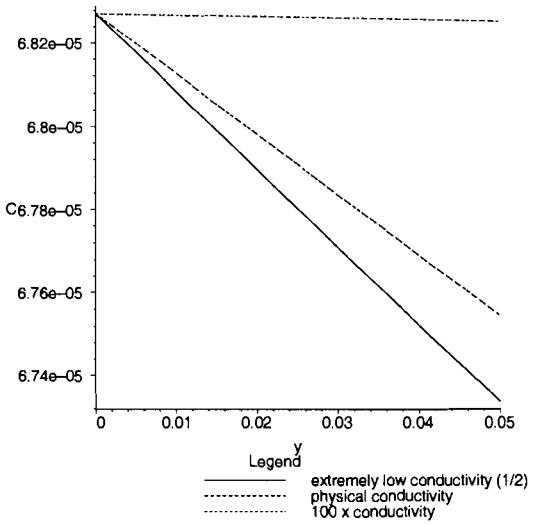

Figure 7.10: The total gas concentration for 3 different thermal conductivity values: $\kappa_s = 5 \times 10^4$, 10^5, 10^7 $erg/cm \cdot s \cdot K$, where I is fixed at 1 Amp/cm^2.

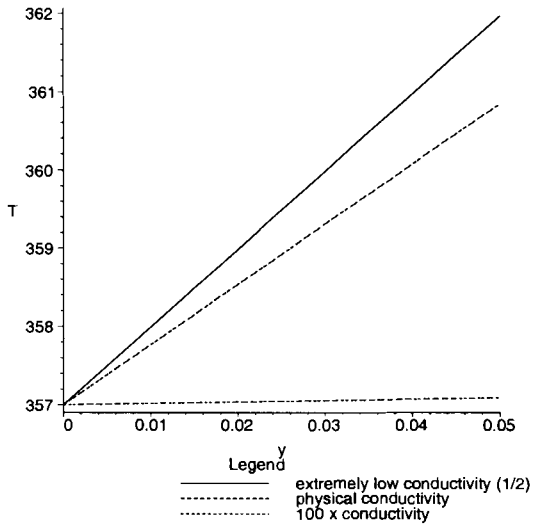

Figure 7.11: The temperature distribution for 3 different thermal conductivity values: $\kappa_s = 5 \times 10^4$, 10^5, 10^7 $erg/cm \cdot s \cdot K$, where I is fixed at 1 Amp/cm^2.

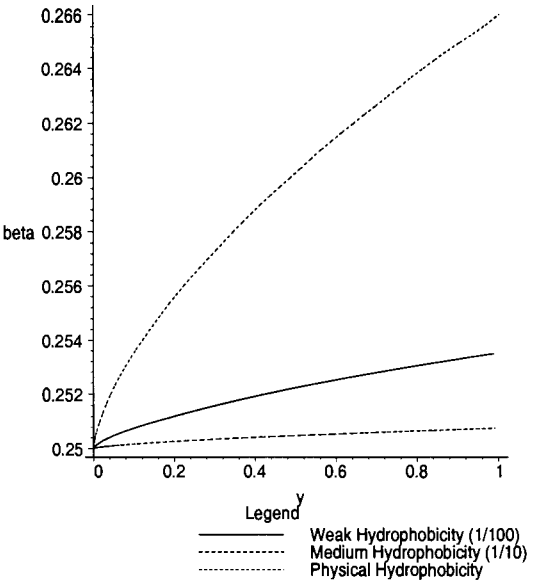

Figure 7.12: The liquid water volume fraction for 3 different hydrophobicity constants: $S_p = 1$, 10, 100, where I is fixed at 1 Amp/cm^2 and κ_s is fixed at 10^5 $erg/cm \cdot s \cdot K$.

7.4 The effects of varying S_p

The final parameter we vary is the hydrophobicity constant, S_p. $S_p = 100$ represents strong hydrophobicity and is the actual value in our model. $S_p = 1$ represents very weak hydrophobicity. As expected, the liquid water volume fraction, β, increases as S_p decreases. This implies that as the GDL becomes less hydrophobic, more liquid water accumulates at the catalyst layer. This study illustrates the importance of the hydrophobic Teflon impregnated in the catalyst layer in order to decrease the amount of liquid water and hence, prevent flooding of the membrane.

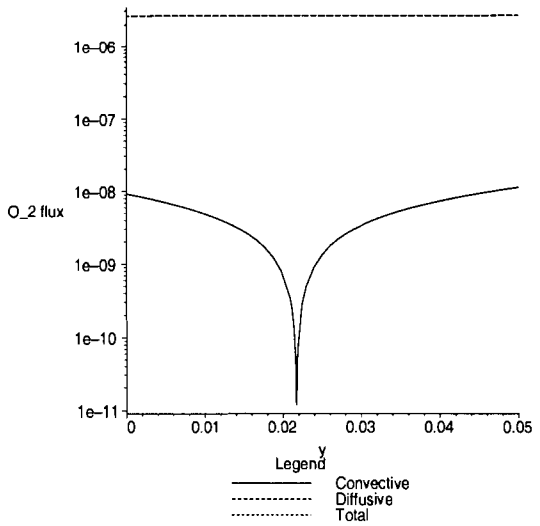

Figure 7.13: The semilog plot of oxygen concentration fluxes (their absolute values) for $I = 1\ Amp/cm^2$, $kappa_s = 10^5\ erg/cm \cdot s \cdot K$.

7.5 The Liquid and Gas Fluxes

Let us now fix $kappa_s = 10^5$, $I = 1$, $T_0 = 1$ and $S_p = 100$ and examine the convective, diffusive and total gas fluxes of the liquid volume fraction and gas concentrations. We observe, in Fig. 7.13 that the total oxygen flux is positive and is therefore toward the catalyst layer. This result is physical - O_2 will flux toward the membrane due to its consumption there. We also observe that the diffusive flux dominates the convective flux. Please note that the absolute value of the convective flux has been plotted and is positive (toward the membrane) until $y \approx 0.02$, then, for $y \in (0.02, 0.05)$, the water fluxes away from the catalyst layer. This result is also physical and can be explained by the condensation effects - which we further explain with the water vapour flux.

The H_2O vapour flux is again shown in a semilog plot in Fig. 7.16 where the diffusive flux is always positive and the convective flux is positive for $y \in (0, 0.02)$ and negative for $y \in (0.02, 0.05)$. Although the convective flux is negligible compared to the diffusive flux, it is an interesting effect to examine. There exists a water sink at $y \approx 0.02\ cm$ as liquid water moves from the channel and evaporates and as water

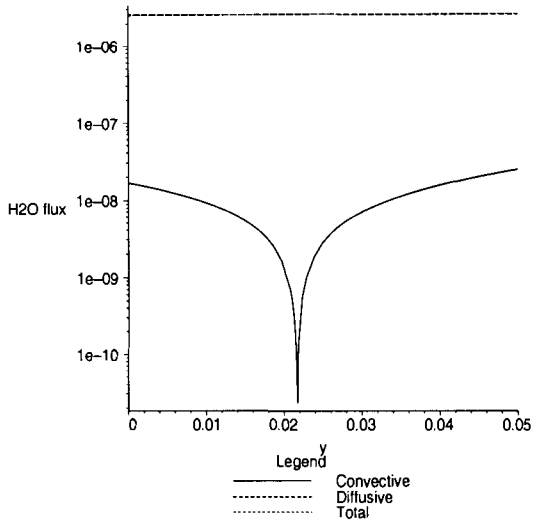

Figure 7.14: The semilog plot of the water vapour concentration fluxes (their absolute values) for $I = 1\ Amp/cm^2$, $kappa_s = 10^5\ erg/cm \cdot s \cdot K$.

vapour produced at the catalyst layer moves toward the channel and condenses.

Figure 7.15 illustrates the total gas flux. Please note that this flux is purely convective. Just as we have seen in the O_2 and H_2O vapour flux, the convective flux is toward the membrane until $y \approx 0.02\ cm$ and then away for $y \in (0.02, 0.05)$. Again, this effect is due to condensation but is also negligible.

In order to further understand the gas movement, let us also examine the total gas velocity, U_g - given in Fig.?? by the second dotted line ($\kappa_s = 10^5$). Just as we observe in Fig. 7.15, the gas velocity due to convection changes direction at $y \approx 0.02\ cm$. We also examine the gas velocity for $1/2$ and 100 times the physical thermal conductivity. As can be seen, if $\kappa_s = 1/2 \times 10^5$, the gas convection is purely toward the channel. If $\kappa_s = 100 \times 10^5$, the gas convection is purely toward the membrane and is no longer a negligible effect.

The phenomenon of changing the direction of U_g with κ_s is shown in Fig.7.17. Please note that κ_s in our model is such that U_g is very small.

Finally, let us also examine the convective, diffusive and total water vapour fluxes when $\kappa_s = 10^7$ (100 times larger than the chosen value). These fluxes are shown in

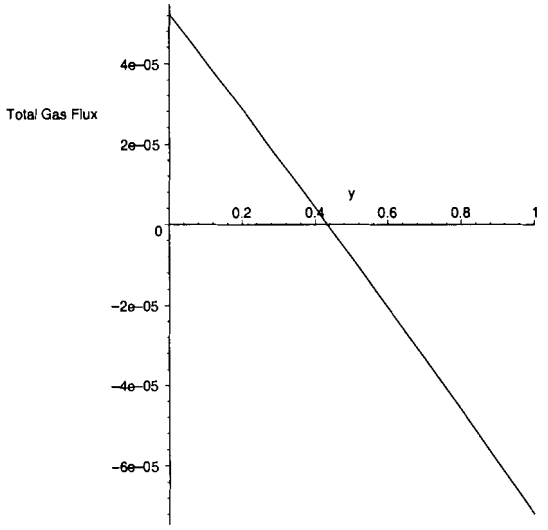

Figure 7.15: The total gas concentration flux for $I = 1\ Amp/cm^2$, $kappa_s = 10^5\ erg/cm \cdot s \cdot K$.

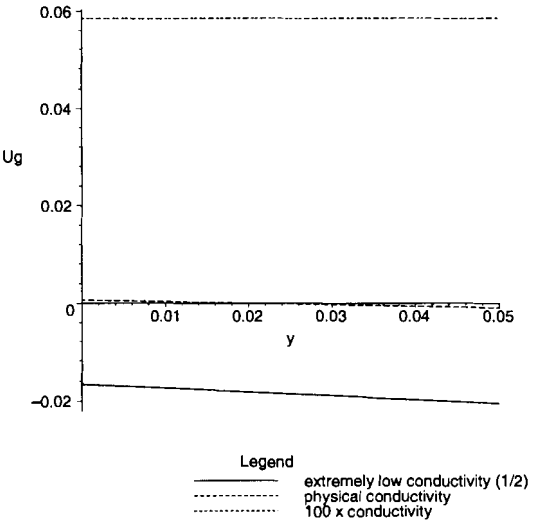

Figure 7.16: The total gas velocity across the GDL for $I = 1\ Amp/cm^2$, $\kappa_s = 5 \times 10^4$, 10^5, $10^7\ erg/cm \cdot s \cdot K$.

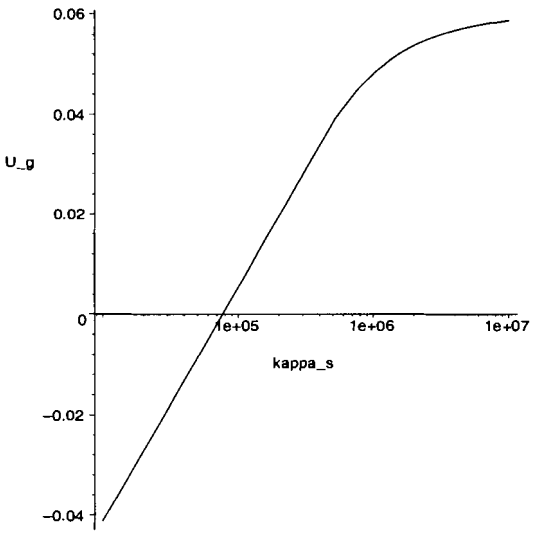

Figure 7.17: The change in U_g with κ_s at the catalyst layer, where $I = 1\ Amp/cm^2$.

Fig. 7.18. Note that now the convective flux dominates and is toward the catalyst layer.

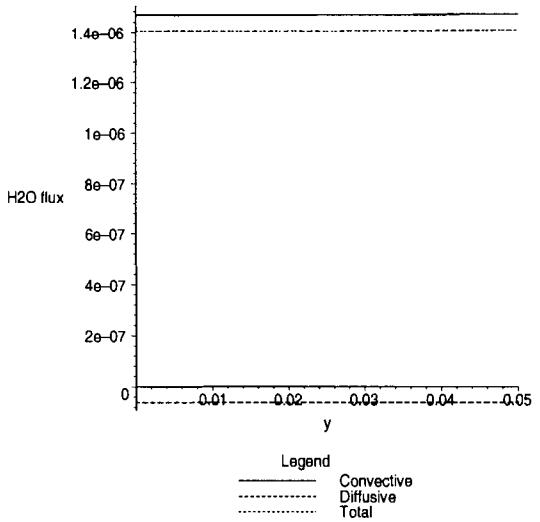

Figure 7.18: The gas velocity with $\kappa_s = 10^7\ erg/cm \cdot s \cdot K$ at the catalyst layer, where $I = 1\ Amp/cm^2$.

7.6 The change in P and Γ with I and κ_s.

Let us finally observe the effects of changing the thermal conductivity and current on the gas pressure correction and condensation rate. Firstly, let us fix $\kappa_s = 10^5$ and vary the current. In Fig.7.19, we see that all the minimum pressures occur at $y \approx 0.02$. This is consistent with the sink that occurs there. Please note that the larger I, the larger the pressure gradient and the more gas flux will occur. This is consistent with the gas profiles seen in Fig.7.4 and Fig.7.6. Next, we will fix $I = 1\ Amp/cm^2$ and vary κ_s. As seen in Fig.7.20, the gas pressure correction is strictly positive (and therefore gas moves away from the membrane) for low conductivities and strictly negative for high conductivities (and the gas movew toward the membrane).

Lastly, let us examine the effects on Γ when we vary the current and the thermal conductivity (seen in figures 7.21 and 7.22). For the physical current value and twice its value, where $\kappa_s = 10^5\ erg/cm\ s\ K$, then $\Gamma < 0$ and the water in the GDL is condensing. For half of the physical current value, we observe that the water is in fact evaporating in the GDL. Finally, as seen in Fig.7.22, for $\kappa_s = 5 \times 10^4$ and 10^5

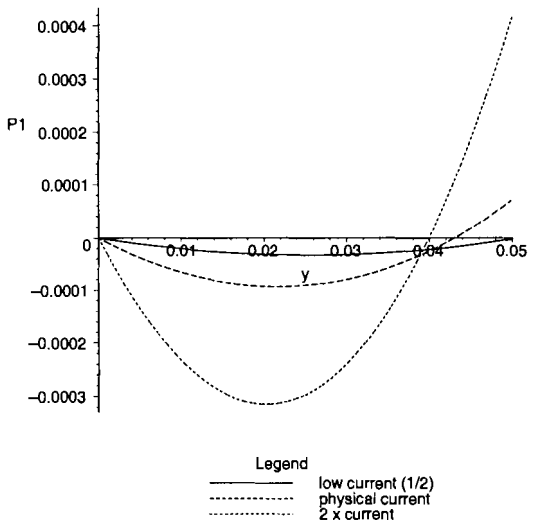

Figure 7.19: The change in the gas pressure, where $I = 1/2,\ 1,\ 2\ Amp/cm^2$ and $\kappa_s = 10^5\ erg/cm \cdot s \cdot K$.

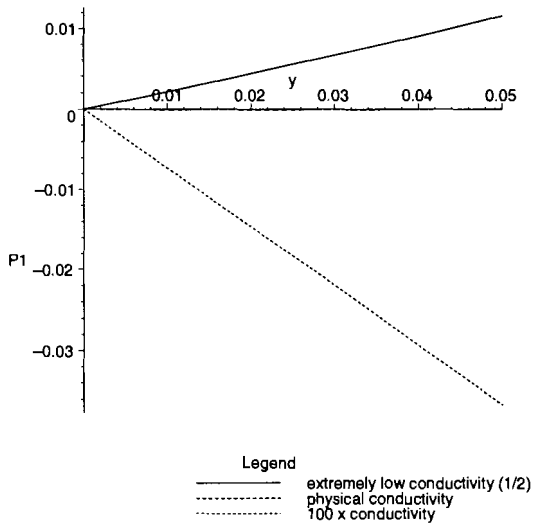

Figure 7.20: The change in the gas pressure, where $I = 1\ Amp/cm^2$ and $\kappa_s = 5 \times 10^4$, 10^5, $10^7\ erg/cm \cdot s \cdot K$.

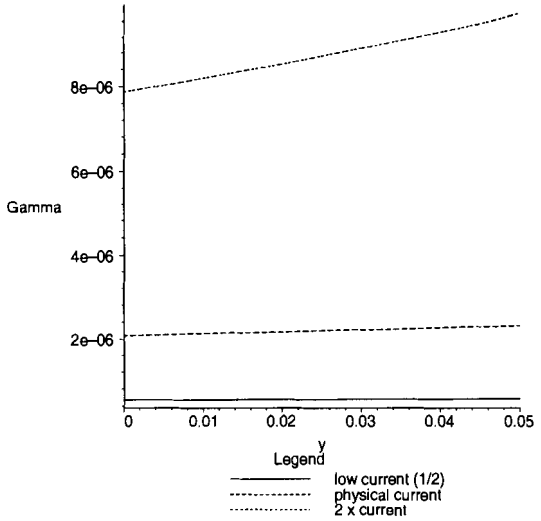

Figure 7.21: The condensation rate where $I = 1/2,\ 1,\ 2\ Amp/cm^2$ and $\kappa_s = 10^5\ erg/cm \cdot s \cdot K$.

$erg/cm\ s\ K$ ($I = 1\ Amp/cm^2$), we observe that water in the GDL is condensing, whereas for $\kappa_s = 10^7$, water is evaporating in the GDL.

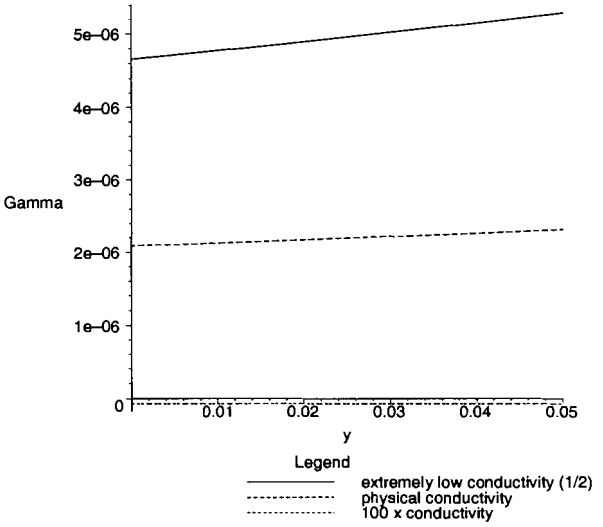

Figure 7.22: The condensation rate where $\kappa_s = 5 \times 10^4$, 10^5, 10^7 $erg/cm \cdot s \cdot K$ and $I = 1$ Amp/cm^2.

Chapter 8

The Conclusions

There are many parameters to be varied in the model presented. Amoungst these, the only three we studied we the current (assumed to be constant) the thermal conductivity, κ_s and the channel temperature, T_0. The most interesting study was to examine the value of ν when these parameters were varied. We can conclude from the studies that ν is very sensitive to changes in the prescribed current and conductivity of the GDL. As a result, all or evn more than 100% of the water produced at the catalyst layer can be condensed with slight changes in the current or thermal conductivity.

We chose a small current, $I = 1\ Amp/cm^2$, which can be called a weak current regime. In this regime, the model gives rise to almost consant values for the gas concentrations, liquid water volume fraction and temperature wwith small derivative terms. Consequently, the gas concentrations and temperature distributions are almost linear.

Finally, we observe that the gas and liquid are convected towards the point $y = 0.02\ cm$ due to condensation but this convective flux is much smaller than the diffusive flux terms for each. This result is consistent with the observation that the phase change has little effect on the gas, temperature and liquid water distributions (Γ is very small in our model).

Chapter 9

Future Work

Our assumption that the GDL is saturated all the way to the membrane, and hence that there is no boundary layer there, implies that we have taken the case $H \gg 1$. The constraint $\Gamma = H(C_2 - C_2^{sat}) = O(1)$ along with the limit $H \gg 1$ imply that $C_2 \approx C_2^{sat}$. An interesting future study would be to allow a boundary layer of width $\frac{1}{H}$ at the membrane. We suppose that the following would be true for this case: water vapour would be convected from the channel to the boundary layer at $y \approx 1 - \frac{1}{H}$, where it would condense. At the same time, the water vapour produced at the membrane would diffuse away from the membrane and condense at $y \approx 1 - \frac{1}{H}$.

Another further study would involve taking all the variables to be time-dependent as well, and solve for the system of equations. An interesting effect to observe would be the water distribution and the amount of humidity at the channel. A question to ask would be, what happens if the channel becomes dry when the GDL cathode is at saturation? From our model, we suppose that the water concentration in the GDL would drop as a result.

Bibliography

[1] L. M. Abriola and G. F. Pinder. A multiphase approach to the modeling of porous media contamination by organic compounds. 1. Equation development. *Water Resour. Res.*, 21(1):11–18, 1985.

[2] J. C. Amphlett, R. F. Mann, B. A. Peppley, P. R. Roberge, and A. Rodrigues. A model predicting transient responses of proton exchange membrane fuel cells. *J. Power Sources*, 61:183–188, 1996.

[3] W. G. Anderson. Wettability literature survey – Part 5: The effects of wettability on relative permeability. *J. Petrol. Technol.*, pages 1453–1468, Nov. 1987.

[4] F. Bagagiolo and A. Visintin. Hysteresis in filtration through porous media. *Z. Anal. Anwend.*, 19(4):977–997, 2000.

[5] P. Berg, K. Promislow, J. Stumper, and B. Wetton. Water management in counter-flowing PEM fuel cells. Submitted to J. Electrochem. Soc., June 2002.

[6] T. Berning, D. M. Lu, and N. Djilali. Three-dimensional computational analysis of transport phenomena in a PEM fuel cell. *J. Power Sources*, 106(1-2):284–294, 2002.

[7] R. P. Bradean, K. Promislow, and B. R. Wetton. Heat and mass transfer in porous fuel cell electrodes. In *Proceedings of the International Symposium on Advances in Computational Heat Transfer*, Queensland, Australia, May 2001.

[8] P. Costamagna. Transport phenomena in polymeric membrane fuel cells. *Chem. Engrg. Sci.*, 56:323–332, 2001.

[9] N. Djilali and D. Lu. Influence of heat transfer on gas and water transport in fuel cells. *Int. J. Thermal Sci.*, 41(1):29–40, 2002.

[10] Teflon industrial coatings: Typical properties. Dupont. http://www.dupont.com/teflon/coatings/typical_props.html.

[11] A. C. Fowler. *Mathematical Models in the Applied Sciences.* Cambridge Texts in Applied Mathematics. Cambridge University Press, 1997.

[12] D. B. Genevey. Transient model of heat, mass and charge transfer as well as electrochemistyr in the cathode catalyst layer of a PEMFC. Master's thesis, Mechanical Engineering, Virginia Polytechnic Institute and State University, Blacksburg, VA, December 2001.

[13] V. Gurau, F. Barbir, and H. Liu. An analytical solution of a half-cell model for PEM fuel cells. *J. Electrochem. Soc.*, 147(7):2468–2477, 2000.

[14] L. Haar, J. S. Gallagher, and G. S. Kell. *NBS/NRC Steam Tables: Thermodynamic and Transport Properties and Computer Programs for Vapor and Liquid States of Water in SI Units.* Hemisphere Publishing Corporation, Washington, DC, 1984.

[15] G. J. Hirasaki. Flow and transport in porous media I: Geology, chemistry and physics of fluid transport. CENG 571 Course Notes, Department of Chemical Engineering, Rice University, 2000. http://www.owlnet.rice.edu/ ceng571.

[16] I.-M. Hsing and P. Futerko. Two-dimensional simulation of water transport in polymer electrolyte fuel cells. *Chem. Engrg. Sci.*, 55:4209–4218, 2000.

[17] G. J. Janssen and M. L. J. Overvelde. Water transport in the proton-exchange-membrane fuel cell: Measurements of the effective drag coefficient. *J. Power Sources*, 101:117–125, 2001.

[18] M. J. Lampinen and M. Fomino. Analysis of free energy and entropy changes for half-cell reactions. *J. Electrochem. Soc.*, 140(12):3537–3546, 1993.

[19] J. Larminie and A. Dicks. *Fuel Cell Systems Explained.* John Wiley and Sons, Chicester, 2000.

[20] C. Lim and C. Wang. Effects of wetting properties of gas diffusion layer on PEM fuel cell performance. In *Third International Symposium on Proton Conducting Membrane Fuel Cells*, Salt Lake City, UT, October 20-25 2002. The Electrochemical Society. Abstract #825.

[21] D. Natarajan and T. V. Nguyen. A two-dimensional, two-phase, multicomponent, transient model for the cathode of a proton exchange membrane fuel cell using conventional gas distributors. *J. Electrochem. Soc.*, 148(12):A1324–A1335, 2001.

[22] H. V. Nguyen, J. L. Nieber, C. J. Ritsema, L. W. Dekker, and T. S. Steenhuis. Modeling gravity driven unstable flow in a water repellent soil. *J. Hydrol.*, 215:202–214, 1999.

[23] K. Promislow, J. Stockie and B. Wetton. Multiphase Transport and Condensation in a Hydrophobic Fuel Cell Cathode. *Private Communication.*

[24] A. Rowe and X. Li. Mathematical modeling of proton exchange membrane fuel cells. *J. Power Sources*, 102:82–96, 2001.

[25] D. Singh, D. M. Lu, and N. Djilali. A two-dimensional analysis of mass transport in proton exchange membrane fuel cells. *Int. J. Engrg. Sci.*, 37(4):431–452, 1999.

[26] M. Slodička. Finite elements in modeling of flow in porous media: How to describe wells. *Acta Math. Univ. Comen.*, 67(1):197–214, 1998.

[27] J. M. Stockie, K. Promislow, and B. R. Wetton. A finite volume method for multicomponent gas transport in a porous fuel cell electrode. *Int. J. Numer. Meth. Fluids*, 41:577–599, 2003.

[28] R. Taylor and R. Krishna. *Multicomponent Mass Transfer.* Wiley Series in Chemical Engineering. John Wiley & Sons, 1993.

[29] W. J. Thomson. *Introduction to Transport Phenomena.* Prentice-Hall PTR, Upper Saddle River, NJ, 2000.

[30] E. A. Ticianelli, C. R. Derouin, A. Redondo, and S. Srinivasan. Methods to advance technology of proton exchange membrane fuel cells. *J. Electrochem. Soc.*, 135(9):2209–2214, 1988.

[31] K. S. Udell. Heat transfer in porous media heated from above with evaporation, condensation, and capillary effects. *J. Heat Transfer, Trans. ASME)*, 105:485–492, Aug. 1983.

[32] S. Um, C.-Y. Wang, and K. S. Chen. Computational fluid dynamics modeling of proton exchange membrane fuel cells. *J. Electrochem. Soc.*, 147(12):4485–4493, 2000.

[33] P. Ustohal, F. Stauffer, and T. Dracos. Measurement and modeling of hydraulic characteristics of unsaturated porous media with mixed wettability. *J. Contam. Hydrol.*, 33:5–37, 1998.

[34] M. I. J. van Dijke and S. E. A. T. M. van der Zee. Analysis of oil lens removal by extraction through a seepage face. MAS Report MAS-R9725, Centrum voor Wiskunde en Informatica, Amsterdam, September 30 1997.

[35] M. T. van Genuchten. A closed-form equation for predicting the hydraulic conductivity of unsaturated soils. *Soil Sci. Soc. Amer. J.*, 44:892–898, 1980.

[36] W. R. Veazey et al., editors. *CRC Handbook of Chemistry and Physics.* CRC Press, 75th edition, 1994.

[37] H. H. Voss, D. P. Wilkinson, P. G. Pickup, M. C. Johnson, and V. Basura. Anode water removal: A water management and diagnostic technique for solid polymer fuel cells. *Electroch. Acta*, 40(3):321–328, 1995.

[38] Z. H. Wang, C. Y. Wang, and K. S. Chen. Two-phase flow and transport in the air cathode of proton exchange membrane fuel cells. *J. Power Sources*, 94(1):40–50, 2001.

[39] N. E. Wijeysundera, B. F. Zheng, M. Iqbal, and E. G. Hauptmann. Numerical simulation of the transient moisture transfer through porous insulation. *Int. J. Heat Mass Transfer*, 39(5):995–1004, 1996.

[40] J. S. Yi and T. V. Nguyen. Multicomponent transport in porous electrodes of proton exchange membrane fuel cells using the interdigitated gas distributors. *J. Electrochem. Soc.*, 146(1):38–45, 1999.

[41] L. You and H. Liu. A two-phase flow and transport model for the cathode of PEM fuel cells. *Int. J. Heat Mass Transfer*, 45:2277–2287, 2002.